7-2018

Force-Driven Weave Patterns for Shell Structures in Architectural Design

Khaled Amir Benaida
University of Nebraska-Lincoln, khaledddd22@hotmail.fr

Force-Driven Weave Patterns for Shell Structures in Architectural Design

By

Khaled Amir Benaida

A THESIS

Presented to the Faculty of

The Graduate College at the University of Nebraska

In Partial Fulfillment of Requirements

For the Degree of Master of Science

Major: Architecture

Under the Supervision of Professor David Newton

Lincoln, Nebraska

July, 2018

Force-Driven Weave Patterns for Shell Structures in Architectural Design

Khaled Amir Benaida, M.S.

University of Nebraska, 2018

Adviser: David Newton

The use of lightweight carbon fiber reinforced polymers (CFRP) in the discipline of architecture opens new possibilities for the construction of architectural components. CFRP has been explored mainly in engineering fields, such as aeronautics, automotive, ballistic and marine engineering. CFRP has also been explored in the discipline of architecture in the construction of shell structures because of its high strength-to-weight ratio and low-cost. There is, however, limited research on how structural analysis can be used to inform weave patterns for shell structures using CFRP.

Further, previous research in the field has not performed physical structural tests to validate which force driven weave patterns perform best. This thesis addresses this gap by contributing a methodology for the creation of CFRP weave patterns from structural analysis and their validation through physical testing. Specifically, this thesis addresses three main problems: Firstly, understanding and analyzing the structural behavior of a shell structure through computation; Secondly, the creation of a weaving pattern of carbon fiber optimized for structural performance; the third part seeks to translate the digital model into fabricated prototypes. The results of this research show that force-flow derived patterns perform best. Consequently, force-flow is the information we should implement to create a more efficient force-driven weave pattern in shell structures.

Acknowledgments

First, I would like to thank David Newton and Timothy Hemsath. Without their guidance, useful critiques, and patience over the past year, this thesis would not have been possible. I would like to thank Nolan Golgert for helping me using the CNC and the shop of the architecture Hall during the summer.

I am eternally grateful to the Fulbright Program for giving me a priceless opportunity to experience a different culture while pursuing graduate studies. I want to thank the AMIDEAST staff for their assistance over the past two years. I would like to acknowledge my sincere gratitude to my friends for their encouragements. I sincerely thank my parents and sisters for their emotional support to overcome my depression.

TABLE OF CONTENTS

LIST OF FIGURES

LIST OF TABLES

LIST OF ACRONYMS

CAD: Computer Aided Design

CFD: Computational Fluid Dynamics

CNC: Computer Numerically Controlled

FRP: Fiber Reinforced Polymers

CFRP: Carbon Fiber Reinforced Polymers

BFRPCS: Basalt Fiber Reinforced Polymers Composite Structures

ICD: The Institute of Computational Design

ITKE: Institute of Building Structures and Structural Design

GA: Genetic Algorithm

PSS: Particle Spring System

FDM: Force Density Method

DR: Dynamic Relaxation

TNA: Thrust Network Analysis

SLS: Selective Laser Sintering

FEA: Finite Element Analysis

FF: Force-Flow

PS: Principle Stress

Chapter 1. Introduction

In recent years, there has been a resurgence in the interest in shells and spatial structures. This is evidenced by several high-profile collaborations between architectural offices and engineers, exploring new optimization methods and innovative materials for the design of shell structures. For example, Massimiliano and Doriana Fuksas developed the New Milan Trade Fair, which refined through numerous computational iterations and resulted in the fabrication of a fluid fabric like canopy (Vinnitskaya, 2012). Another example can be found in the design of the Shenzhen Bao'an International Airport, which was designed as a double-layered skin that allows the infiltration of natural light (Vinnitskaya, 2012). Also, Toyo Ito and Mutsuro Sasaki designed the crematorium of Kakamigahara using computational morphogenesis and genetic algorithms (GA) to find the best solution for the design. These examples demonstrate the use of computational design processes to address the complexity of modern shell structure design.

The inclusion of fiber-reinforced polymer (FRP) materials in shell structures offer substantial potential due to their high strength-to-weight ratio (Menges et al), durability, thermal performance, low-cost, and their ability to create a dynamic range of forms. (Simon et al. 2016) for example, argue that composite systems in architecture are no longer constrained by pre-established parameters such as the shape, size, and traditional construction techniques, but rather offer a holistic approach where a continuous winding technique can fabricate the entire building without the need for molds. Many scholars and institutions in Europe and the U.S have recently turned to FRP, especially the employment of carbon fiber and fiberglass, as a new lightweight material for shell structures. The Institute of Computational Design (ICD) and the Institute of Building Structures and

Structural Design (ITKE) in Stuttgart have done extensive interdisciplinary research on carbon fiber reinforced polymers (CFRP). The ICD has produced several research pavilions exploring CFRP as a building material. Their 2013-14 pavilion uses a biomimicry-based approach to inform the design of a highly articulated material system of CFRP. In their 2014-2015 research pavilion, they mimicked the behavioral patterns of a spider's shelter and self-fabrication of the shell. This project was constructed by implementing a pneumatic formwork of ETFE erected on a plywood base, and then carbon fibers and resin were added on the pneumatic surface with a 6 -axis robot arm. The research of (Menges et al.2015) demonstrate that fibrous structures can produce multiple performative qualities such as flexibility and differentiated structural reinforcement.

This precedent research shows that CNC weaving provides some distinct advantages in the fabrication of double-curved surfaces. The precedent work explored the principal stress as the main driver to create a weave pattern in shell structures. Therefore, this research seeks to understand the difference between force flow and principal stress lines in shell structures and validate which weave pattern is the most efficient.

1.1 Contributions

This research contributes knowledge on the application of structural analysis to the development of structurally efficient CFRP weave patterns for shell structures. Specifically, the research explores the use of two different approaches to produce structurally optimal weave patterns and through physical tests determines which approach is most efficient.

Chapter 2. Literature Review

An important focus of this thesis is the efficient fabrication and optimization of shell structures. This chapter, therefore, begins with a history of shell structures. That history explores how the design and fabrication of these structures evolved in the field of architecture and the methods that were developed over time for their structural optimization. That history covers how these structures progressed starting from their construction with masonry during the middle ages; to their materialization in reinforced concrete in the 1950's and 1960's; and finally, to their fabrication with FRP and CFRP in the contemporary era.

This chapter also reviews the methods of structural optimization used for the design of shell structures in the 20th and 21st century. Specifically, it summarizes form-finding processes and other methods of optimization. The section ends with a review of precedent optimization examples involving force-driven weave patterns.

2.1 History of Shell Structures

Shell structures are one of the oldest forms investigated by architects to create long-span structures. In ancient Rome, the romans used masonry and concrete to create a number of impressive shell structures, such as the Coliseum, the Pantheon, and Pont du Gard in France. Cathedrals and ceremonial palaces in Europe from the middle ages and the Renaissance are also examples of these structures, including Exeter Cathedral and King's College Chapel in Cambridge. In the late 19th century, Rafael Guastavino Moreno invented the Catalan vault and the Guastavino tile which would be used famously in the Boston Public Library and the Grand Central Terminal in New York City, and. In the early 20th century, Antoni Gaudi created a number of impressive shell structures using analog form-

finding shells (Weller 2010). He pioneered analogue form-finding to find structurally optimized forms (e.g, Colonia Guell Church, and Casa Mila) (Weller 2010). Form finding is the process of finding structurally efficient shapes by allowing parametrically constrained material systems to self-organize into minimum energy configurations.

The first steel-reinforced concrete shells appeared in the 1950's and 1960's. This time is often referred to as the era of structural expressionism (Sasaki 2014). With the advancement of research in the chemical makeup of concrete, the usage of spray-applied concrete (shotcrete), precast, and reinforced concrete enabled architects to build faster and less expensive buildings. The principal actors of this era were mostly engineers who were interested in designing economical long-span structures. In Figure 2.1, two examples are shown from this period by Felix Candela and Pier Luigi Nervi.

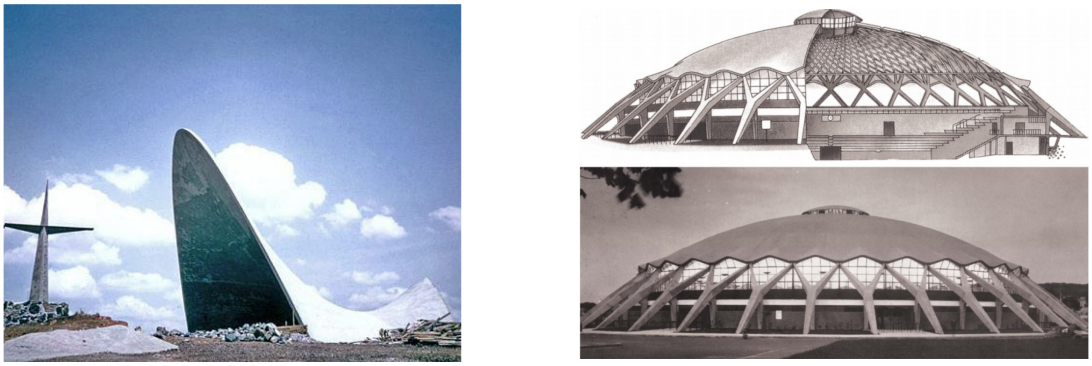

Figure 2.1. Chapel Lomas de Cuernavaca by Felix Candela (left), and Palazzetto dello Sport by Pier Luigi Nervi, Rome (right). Retrieved from: http://customrodder.forumactif.org/t4351-chapel-lomas-de-cuernavaca-mexico-architect-felix-candela

Another notable example can be found in the work of the architect and engineer Frei Otto, who developed innovative and economic tensile structures using form-finding methods involving soap films. This work was done at the Institute of Lightweight Structures at the University of Stuttgart. Figure 2.2. The scale model studies used by Frei Otto to study the forces in a cable net shell (Weller 2010).

Other distinguished shell structures designed by Frei Otto include the Munich Olympic Stadium completed in 1972; the West German Pavilion at Expo 67, completed in Montreal in 1967; the Multihalle in Mannheim completed in 1975; the Tuwaiq Palace in Saudi Arabia, completed in 1985.

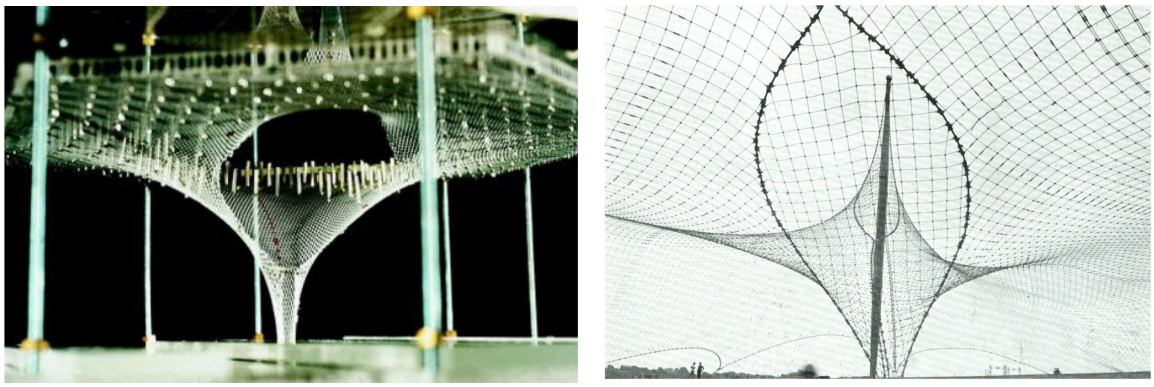

Figure 2.2. The scale model studies used by Frei Otto to study the forces in a cable net shell (Weller 2010). Retrieved from: https://www.pinterest.com/pin/435160382721782751/

Concrete shells are rarely constructed today because of the scarcity of skilled workers; rising prices for formwork; cost and schedule challenges; and the inefficiency of on-site fabrication (Sasaki 2014). In the early 1990's, the development of new computational tools allowed architects like Norman Foster to implement nonlinear computer analysis using Dynamic Relaxation (DR) for the structural analysis of the British Museum's grid shell roof, as shown in Figure 2.3 (Williams 2014). Similarly, Massimiliano Fuksas conceived Myzeil's facade in Frankfurt, it was designed by alternating panels of glass and steel as shown in Figure 2.4.

Figure 2.3 The British museum grid shell designed by Norman Foster. Retrieved from: https://www.fosterandpartners.com/projects/great-court-at-the-british-museum/

Figure 2.4 Myzeil's facade in Frankfurt was designed by alternating panels of glass and steel by Massimiliano Fuksas. *Retrieved from: https://www.archdaily.com/243128/myzeil-shopping-mall-studio-fuksas*

The emergence of more powerful and readily available computational performance analysis and optimization tools from 2000-2018 has further increased interest in the design of shell structures. For example, innovative research on FRP applied to shells by Zaha Hadid Architects demonstrated that optimization could be used to make affordable yet complex shell structures. The optimization required the shape to be tessellated to create serial compartments of double and single curve forms of the building envelope. Figure 2.5 shows the tessellated skin of Heydar Aliyev Center (left); and Chanel Mobile Art Pavilion (right) designed by Zaha Hadid Architects.

Figure 2.5 The tessellated skin of Heydar Aliyev Center (left); and Chanel Mobile Art Pavilion (right) designed by Zaha Hadid Architects. Retrieved from: http://www.zaha-hadid.com/architecture/heydar-aliyev-centre/

2.1.1. Fiber Composites Shell Structures

This section discusses how FRP was employed in architecture chronologically. In the 1970s, FRP composite structures started to be used as a building material (Berardi et al. 2015). By the mid-1980s it was mainly used in reinforced concrete or as a structural material in aggressive and hostile conditions (Berardi et al. 2015). Until the 1990's, it was partially used in the construction (Berardi et al. 2015). Recently the use of FRP in shell structures have been increased. For example, the One Ocean pavilion designed by SOMA for the 2012 Expo in South Korea is an example of this new trend, as shown in Figure 2. 6, the façade of this building has a large FRP louvers which were used to mitigate sunlight (Berardi et al. 2015).

Figure 2.6 One Ocean Pavilion for South Korea Expo 2012 designed by SOMA (Berardi et al 2015). Retrieved from: http://mdpi.com/2073-4360/7/11/1513

A less successful recent example is *La médiathèque de Pau* in France designed by Zaha Hadid Architects with the collaboration of Marc Fornes. Figure 2.7 shows the project, which is constructed using pre-preg carbon fiber, epoxy and sandwich panels. The project failed to fulfill the budget and technical specifications because the skin was entirely developed in carbon fiber. Consequently, the local authorities canceled the project because

of its exuberant character and cost, which exceeded initial budget by two times (Fornes 2014).

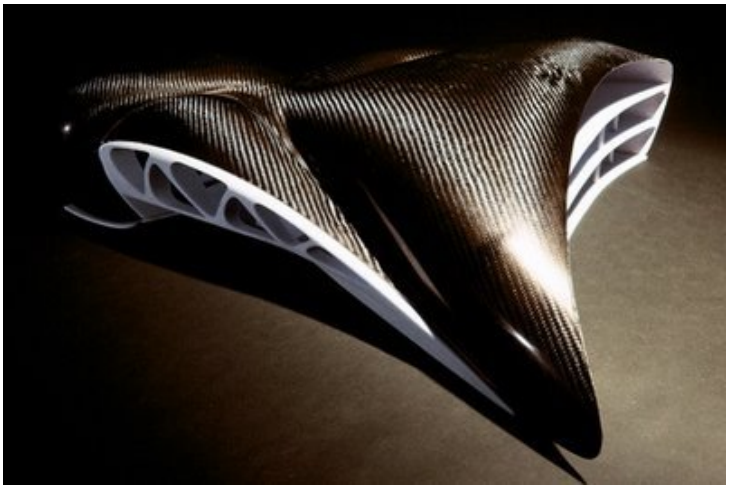

Figure 2.7 La médiathèque de Pau designed by Zaha Hadid Architects (Fornes 2014). Retrieved from: https://theverymany.wordpress.com/at/zaha-hadid-architects/

One important area of research on shell structures involves alleviating the need for expensive formwork to make shell structures. An experimental research project by (Blonder 2015) focused on an alternative fabrication process in FRP by making a mold free process, using form-finding with fabric hardening techniques of FRP (Fiber reinforced polymers) (Blonder 2015). They used two different design software tools: Grasshoper/Kangaroo and 3ds max. In addition to computational research, they inverted a medium-large pre-preg carbon fiber fabric painted with resin measuring 200 cm x 1000 cm x 100 cm (Blonder 2015).

Another FRP research prototype shown in Figure 2.8 is called the Pleated Shell Structure and was designed by Zaha Hadid and exhibited at the South California Institute of Architecture. The project consists of stretching fabric to define minimal surface geometries with the use of wood boundary conditions. This avoids the need for molds. The team of ZHA created the shape by dividing the form into different compartments; they added the resin and the fiberglass to harden the fabric and assemble the parts once the resin was cured (Schumacher, 2012).

Figure 2.8 The Pleated Shell Structure designed by Zaha Hadid Architects and exhibited at Sci-arc. Retrieved from: https://www.e-architect.co.uk/losangeles/sci-arc-architecture-news

An FRP research project by (Corazza 2014) focused on the use of a geometrical framework based on sandwich materials and the bending behavior of a core material made of thermoplastic foam. The aim of the research was to overcome the need for extensive formwork. The project was designed as an emergency shelter for storms. They implemented a GA to optimize the design for structural efficiency, taking into consideration environmental inputs like wind and water pressure.

The Institute of computational design (ICD) with the collaboration of ITKE at the University of Stuttgart has also developed a large body of multidisciplinary research on FRP and CFRP shell structures. Specifically, their research combines the disciplines of biology, engineering, and architecture to develop novel construction processes to create shell structures. Their research starts by analyzing natural systems and then translates principles from these natural precedents into highly articulated CFRP shell structures. For example, their 2013-14 research pavilion started by analyzing the structure of eight different flying beetles and extracted principles on density patterns and fibers arrangements to inform the creation of a CFRP pavilion (Menges et al 2014). The entire structure was composed of 36 modules of double layer core-less carbon fiber and fiberglass. To achieve a highly efficient distribution of fibers across the structure, the integration of reliable robotic fabrication and performance analysis processes was necessary (Menges et al 2014). Figure 2.9 shows the final ICD pavilion in Stuttgart that highlights this biomimetic investigation.

Figure 2.9 The final ICD pavilion 2013-14 in Stuttgart. Retrieved from: https://www.archdaily.com/522408/icd-itke-research-pavilion-2015-icd-itke-university-of-stuttgart

The ICD 2014-15 research pavilion tried to mimic the underwater nest construction of the Agyroneda Aquatica water spider. The pavilion was fabricated by implementing a pneumatic formwork of ethylene tetrafluoroethylene, or ETFE, erected on a plywood base. The carbon fiber patterns were created by using a computational agent-based design. The fibers were fabricated with the use of a 6-axis robot arm (Menges et al 2014). Figure 2.10 shows the process of fabrication of the pavilion (Menges et al 2014).

Figure 2.10 Robotic fabrication from the inside of the ETFE shell, robot arms lays carbon fibers by using a computational agent-based design (Menges et al 2014). Retrieved from: https://www.designboom.com/architecture/icd-itke-research-pavilion-2014-15-water-spider-07-16-2015/

In summary, the research on the fabrication of shell structures using FRP winding technique is a solution of making a holistic and comprehensive technique to avoid the dependency on formwork and the lengthy assembly process in shell structures. FRP material can alleviate the heavy and costly process of the execution of shell structures. Current research however did not address the problem of how to translate the digital FEA to weave pattern, they did not explain how they inform the path of the weave pattern. My research addresses this gap by contributing to test a difference between force flow lines and principal stress lines generated by the FEA software.

2.2 History of Form Optimization Methods Based on Structural Information

This section reviews a brief history of form optimization based on structural information. It starts by reviewing the application of form-finding in shell structures throughout the 20th and 21st centuries. In this review, both analogue and computational form-finding techniques are discussed. The section concludes with a brief overview of precedent work involving force-driven CNC weave patterns for shell structure design.

2.2.1 Analogue Form-Finding

There are several form-finding methods for shell structures: hand calculation with graphic statics and vectors; computational approaches; and form-finding through physical prototyping. The aim of form-finding is to find the form and the thickness distribution of a shell for specific functional requirements, such as boundary conditions; multiple load cases; and material properties (Ekkehard Ramm 2014).

A hanging model was the first simulation tool of a family of structures known as funicular structures (tension or compression only). When a chain is suspended between two points, it will form a V shape, and each element along the chain will be in perfect tension. When that chain is then inverted, it will create an ideal compression structure (Weller, 2010). Robert Hooke (1635-1703) was the first scientist who introduced this experiment (Block et al. 2014). Figure 2.11 shows a hanging model of the Cripta de la Colònia Güell by, near Barcelona, Spain in 1915 (Rippmann 2016) and an inverted photograph of a poly-funicular model for study of the structure of a church, by Antoni Gaudi (Block et al 2014). Figure 2.12 shows Poleni's analysis of the Dome of St.-Peter's in Rome, Italy (1748) using two-dimensional hanging string models (Block et al. 2014).

Another noticeable example of analog form-finding methods that characterized the 20th century was Heinz Isler research as shown in Figure 2.13.

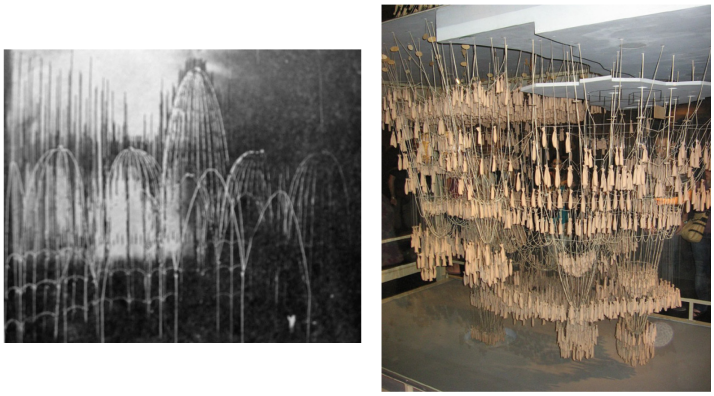

Figure 2.11. The funicular model of the Colonia Güell (right), and a funicular model of a church, by Antoni Gaudi (Block et al 2014). Retrieved from: https://moreaedesign.wordpress.com/2010/09/13/more-about-sagrada-familia/

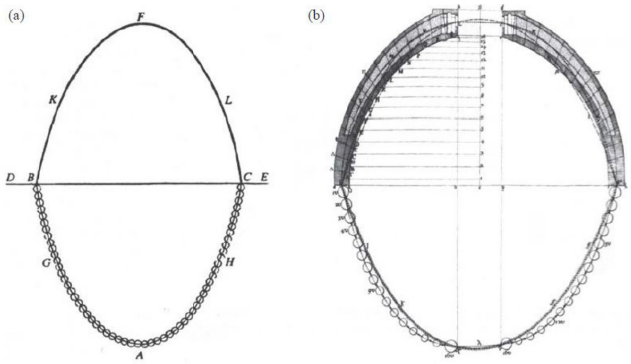

Figure 2.12 the analysis of the Dome of St.-Peter's in Rome (1748) (right image) (Block et al 2014) (left image) Drawing of Hooke's analogy between an arch and a hanging chain. Retrieved from: https://www.researchgate.net/figure/a-Polenis-drawing-of-Hookes-analogy-between-an-arch-and-a-hanging-chain-and-b-his_fig1_225587685

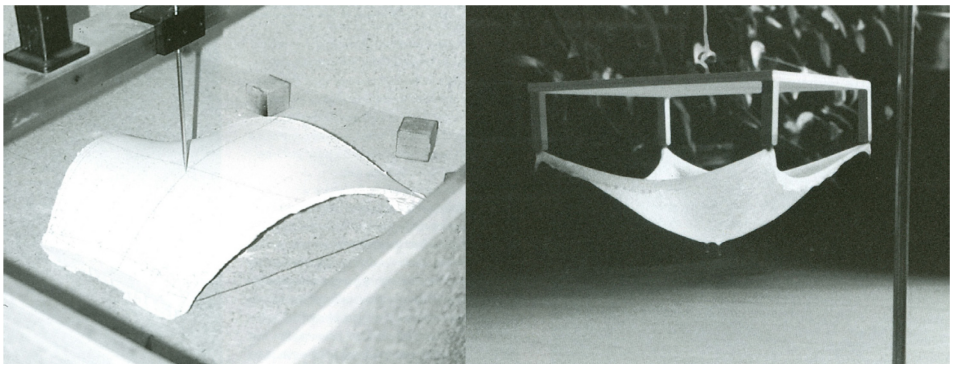

Figure 2.13 Isler's models of an inverted surface (left) and then the calculation of forces (right) (Weller, 2010). Retrieved from: http://formactive.pbworks.com/f/MWeller_Proposal_9-26.pdf

2.2.2 Computational Form-Finding

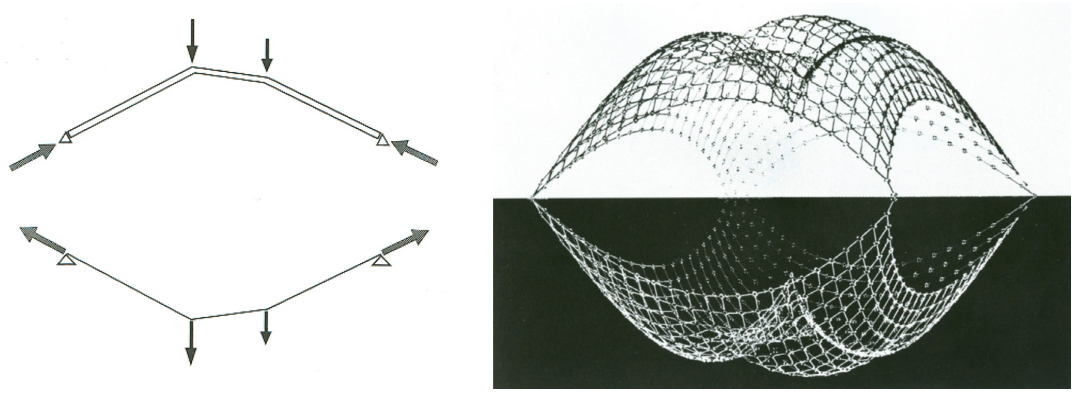

Figure 2.14 A diagram shows the inverted string and the loads applied to it (left); Frei Otto also used this technique to experiment in Stuttgart(right) (Weller, 2010). *Retrieved from: http://formactive.pbworks.com/f/MWeller_Proposal_9-26.pdf*

In the early 1990's, form-finding processes were digitalized using CAD programs. These programs were tailored for the needs of the construction industry and considerably reduced the amount of time that physical form-finding methods experimented by Frei Otto as shown in Figure 2.14. Computational methods use boundary settings and the preset loads as the key factors taken into consideration for the study of form-finding. There are two points of departure for these methods: the first one is purely graphic using graphic statics like the thrust network analysis (TNA); the other one is exclusively analytical such as force density method (FDM), particle spring system (PSS), dynamic relaxation (DR), and computational morphogenesis (Block et al. 2014).

2.2.3 Particle-Spring System (PSS)

Most algorithms and computational software for form-finding use particle-spring systems. According to Ochsendorf and Axel Kilian "The PSS method is practical because the designer can make modifications of the shape and forces in real time while the solution is still emerging" (Block et al 2014). Further, Weller argues that "Particle-spring systems contain two main elements: particles and springs. Particles (nodes) are assigned position and mass values, while springs (bars) are given a strength value, a rest length, and two particles, which they serve to connect" (Weller 2010). The principal purpose of the particle-spring method is to find structures in static equilibrium. This objective is achieved by defining the topology of a particle spring network with loads on the particles, the masses of the particles, the stiffnesses and lengths of the springs, and then by attempting to equalize the sum of all forces in this system (Block et al 2014). Figure 2.15 shows Bangalore shell designed by Zaha Hadid Architects; they used PSS as a form-finding process in this project (Bl

Figure 2.15 On-site fabric guide work for Bangalore shell designed by Zaha Hadid Architects, AA Visiting School in India 2011 (Block et al 2014) Retrieved from: http://www.zha-code-education.org/AA-VISITING-SCHOOL-INDIA-DELHI-JULY-2013

2.2.4 Force Density Method (FDM)

According to Klaus Linkwitz "The force density method can generate solutions of discrete networks, through a linear system of equations that are in the exact state of equilibrium." Linkwitz said that "The FDM technique was designed originally for cable nets; it is commonly used to calculate tensioned fabric roofs, especially synclastic (dome-shaped) structures" (Linkwitz. 2014). The use of FDM demonstrates a method for rapid generation of possible shapes for prestressed and inverted hanging structures. This form-finding method allows the quick exploration of effective solutions without knowing the material properties of the project, which is especially useful in the early stages of a project (Linkwitz 2014). The force density method does not require any knowledge of the structure. (Linkwitz. 2014). Figure 2.16 shows Solemar Therme Bad Durrheim, completed in 1987, designed by Frei Otto. FDM was used for this project (Linkwitz. 2014). Figure 2.17 shows a timber shell roof of the 1974 Mannheim Multihalle, designed by Frei Otto (Linkwitz. 2014).

Figure 2.16 Solemar Therme Bad Durrheim, 1987. Retrieved from: https://www.gesundheitszentrum-solemar.de/infos/solemar-therme/

Figure 2.17 Timber shell roofs of the 1974 Mannheim Multihalle designed by Frei Otto (Linkwitz. 2014) Retrieved from: http://www.fastepp.com/index.php/en/projects-2/current/multihalle-in-mannheim

2.2.5 Dynamic Relaxation (DR)

Alistair Day introduced dynamic relaxation in 1965 and it is a numerical procedure that solves a set of nonlinear equations (Williams et al 2014). For example, Norman Foster's Smithsonian project uses dynamic relaxation to produce and even spacing between the structural grid. DR was also used in the design of the British museum gridshell (Williams et al 2014).

2.2.6 Thrust Network Analysis (TNA)

According to Philippe Block, the Thrust Network Analysis (TNA) method uses graphic statics as a foundation of form-finding. Block argues that the form diagram represents the overall shape and the geometry of the 3D thrust network projected in the plan, while the force diagram shows the magnitude of forces according to the form diagram, and each vector in the form diagram is drawn to scale in the force diagram (Block et al 2014). Figure 2.18 shows four diagrams: a masonry arch of arbitrary geometry with a thrust line (e.g., part 'a' of the diagram); and corresponding hanging string (e.g., part 'b'); the force diagram (e.g., part'd') showing the equilibrium of one stone block (Block et al 2014). The topological and geometrical relationship between the two graphs is reciprocal, meaning that the form can drive the force and vice versa, we cannot separate them. The final resolution of the 3D form is called the thrust network (Block et al 2014) as shown in Figure 2.19.

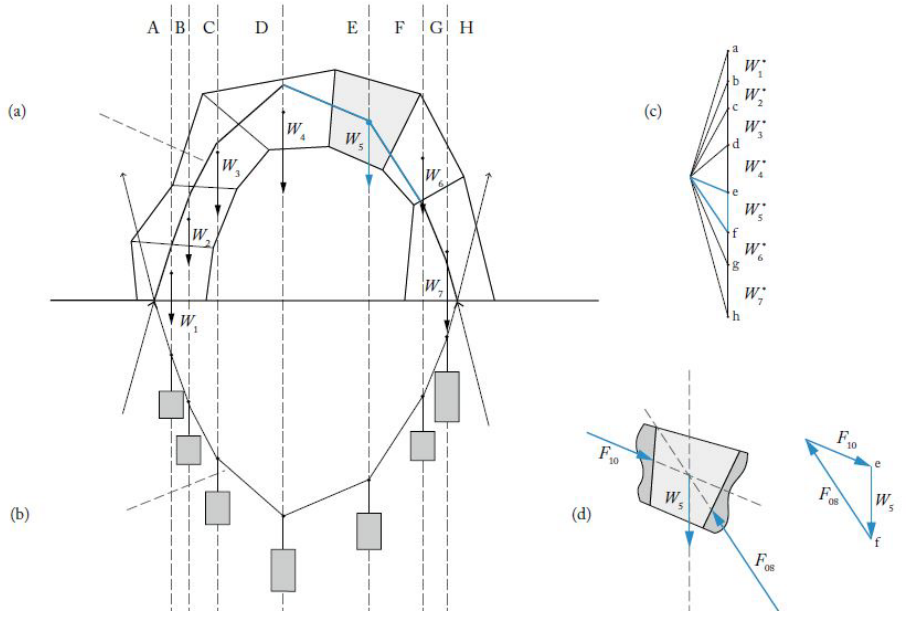

Figure 2.18 Global and local force vector equilibriums in the funicular line (Block et al 2014) Retrieved from: http://web.mit.edu/masonry/papers/block_SMArchS_2005.pdf

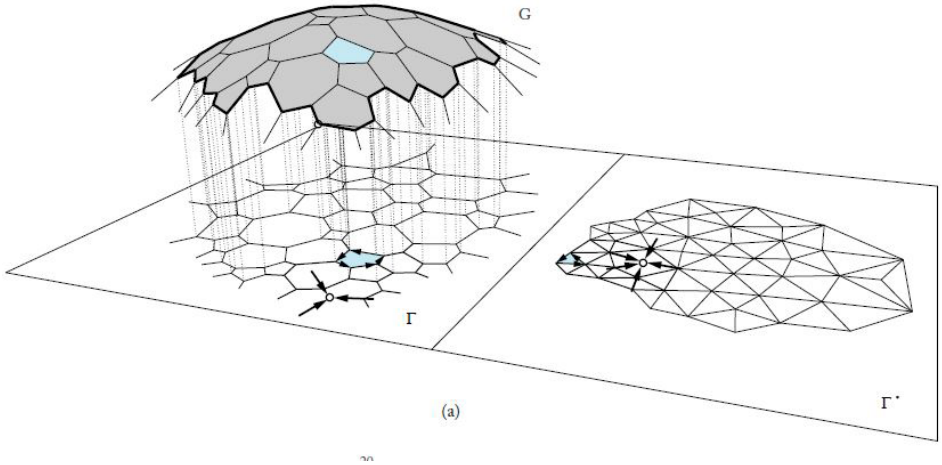

Figure 2.19 (a) Relationship between the thrust network G, its planar projection, the form diagram Γ and the reciprocal force diagram Γ (Block et al 2014) **Retrieved from:** *https://www.researchgate.net/publication/237684255_Thrust_network_analysis_A_new_methodology_for_three-dimensional_equilibrium*

2.2.7 Force-Driven Weave Patterns in Shell Structures

This section identifies different research projects that use structural analysis as a main driver to create weave patterns in shell structures. A notable project in this area by Zaha Hadid Architects is the CIAB Pavilion. It was done in collaboration with Bollinger and Grohmann for the China International Architectural Biennial. In the project, Felix Candela's complementary hypar shells were reinterpreted using multi-objective evolutionary algorithms as a parametric investigation. They used principle stress as a main driver for structural weave pattern (Karamba 3d, CIAB Pavilion 2018). Then they translated the stress pattern into a double layer of steel pipes (Karamba 3d, CIAB Pavilion 2018). Figure 2.20 shows Candela's pavilion revisited, by Zaha Hadid Architects.

Figure 2.20 Zaha Hadid Architects pavillion for the CIAB 2013 Retrieved from: https://www.karamba3d.com/projects/ciab-pavilion/

The Institute of Computational Design (ICD) at Stuttgart did another notable speculative pavilion in 2013-14. FEA was used to visualize the structural performance of the global geometry. Figure 2.21 shows a structurally differentiated winding development diagram for the project. In the project, carbon fibers were placed according to the force vectors and their amplitude and direction (Menges et al. 2014). Although the project demonstrated the fabrication of a highly efficient lightweight structure, the research lacked explanation about how structural data was being used to inform not only the weave pattern

but also the density. This was also the case for the ICD's 2014-15 research pavilion shown in Figure 2.22, which expanded integrative design methodologies by including sensor data and real time robotic control, allowing for design adaptability during the placement of carbon fibers (Dörstelmann Moritz 2014).

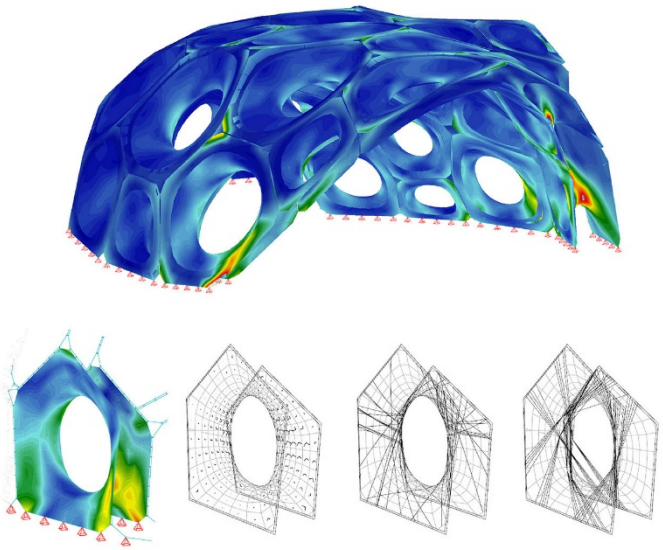

Figure 2.21 Finite element analysis of 2013/14 ICD Pavilion and the translation of structural analysis to carbon fibers (Dörstelmann Moritz 2014 et al). Retrieved from: https://www.designboom.com/architecture/icd-itke-research-pavilion-2013-14-interview-08-18-2014/gallery/image/icd-itke-research-pavilion-stuttgart-2014-designboom-9/ http://ada.gov.

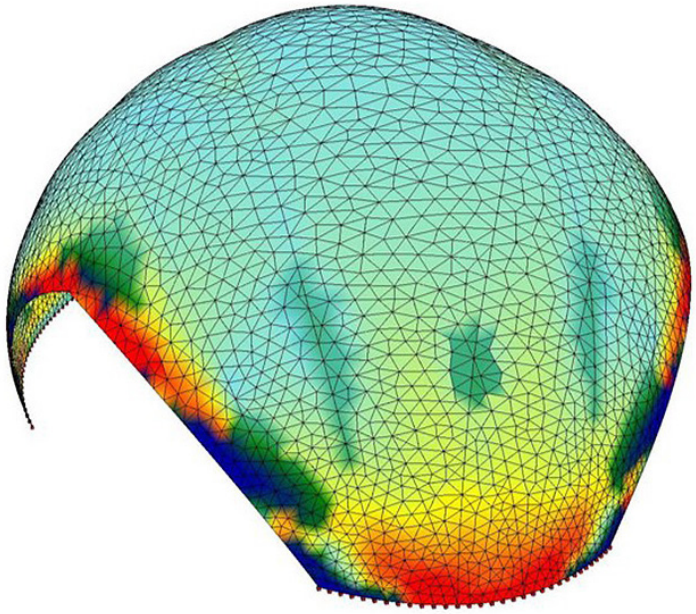

Figure 2.22 Finite element analysis of 2014/2015 ICD Pavilion. Retrieved from: http://icd.uni-stuttgart.de/?p=12965

In summary, the research on CFRP applied to shell structures has focused only on the use of principal stress information to create structurally optimal weave patterns. This is demonstrated in the CIAB pavilion done by Zaha Hadid and ICD's 2014-15 pavilion. The research in this thesis directly addresses this issue and contributes knowledge in this area by comparing the use of weave patterns derived from principal stress verses using other structural information, such as force flow vectors.

Chapter 3. Methodology

This section describes the process of translating structural performance analysis into specific weave patterns for shell structures. Then it outlines an experimental set-up in which the structural efficiency of these weave patterns is tested on three different forms: a double-curved positive Gaussian shell form; a double-curved negative Gaussian form; and a single-curved zero Gaussian form. Lastly, the translation of these weave patterns into physical prototypes through subtractive and additive fabrication processes for structural testing is discussed.

3.1 Digital Structural Analysis

The structural analysis is a process that gives us a clear understanding of behavior and performance of the structure under a specific set of parameters, such as the load; the form of the structure; the boundary conditions; and the material properties of the structure. In this research, computational finite element analysis is used to generate information about structural performance instead of hand calculations. Specifically, Rhinoceros 3D and its parametric plug-in Grasshopper is used to generate the forms, while the Karamba structural analysis plugin for Grasshopper is used for the digital structural analysis as shown in Figure 3.1. Karamba was chosen because of its availability to students. Some examples of projects used Karamba as FEA tool of investigation include the Candela Pavilion at China International Architectural Biennial

(CIAB) in Beijing, China, ad designed by Zaha Hadid as shown in Figure 2.20. In addition, Figure 3.2 shows white noise project designed by soma architecture

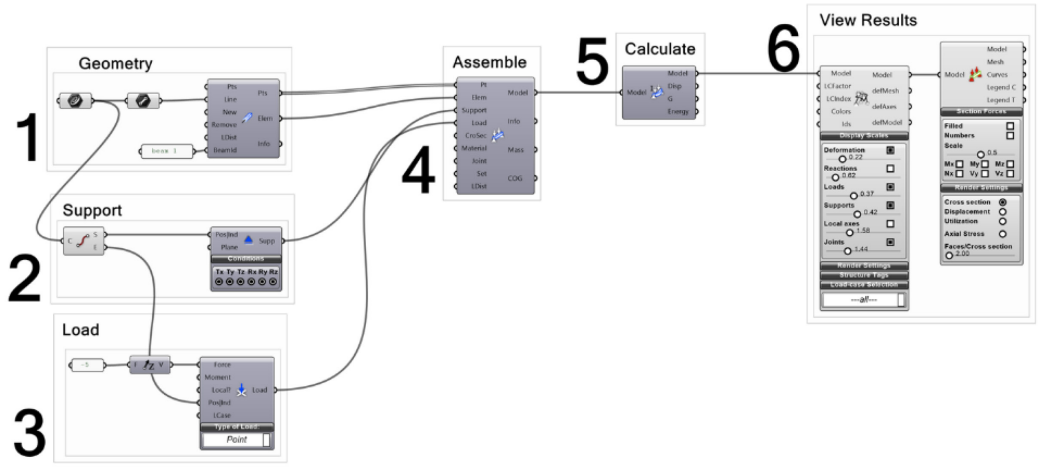

Figure 3.1 A screenshot of a simplified workflow diagram of structural analysis using Grasshopper/Karamba,it explaipons each step in the process. 1 Geometry, 2. Support, 3 Load, 4 Assemble, 5 Calculate, 6 View Results. **Retrieved from: http://ada.gov.**

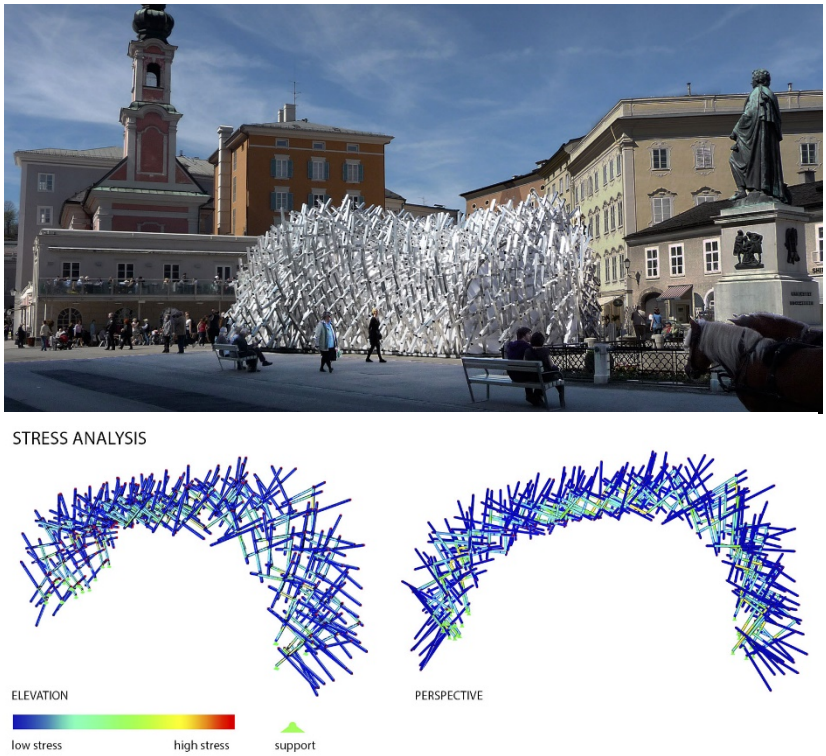

Figure 3.2 White noise designed by soma architecture and Bollinger+ Grohmann, Salzburg, Austria. (Karamba 3d, CIAB Pavilion 2018). Retrieved from: https://www.karamba3d.com/projects/white-noise/

This research investigates three different possible shell structure forms: positive Gaussian curvature (Synclastic) forms, negative Gaussian curvature (anticlastic) shells, and shells with zero Gaussian curvature. Figure 3.3 shows the general diagram of the digital structural analysis.

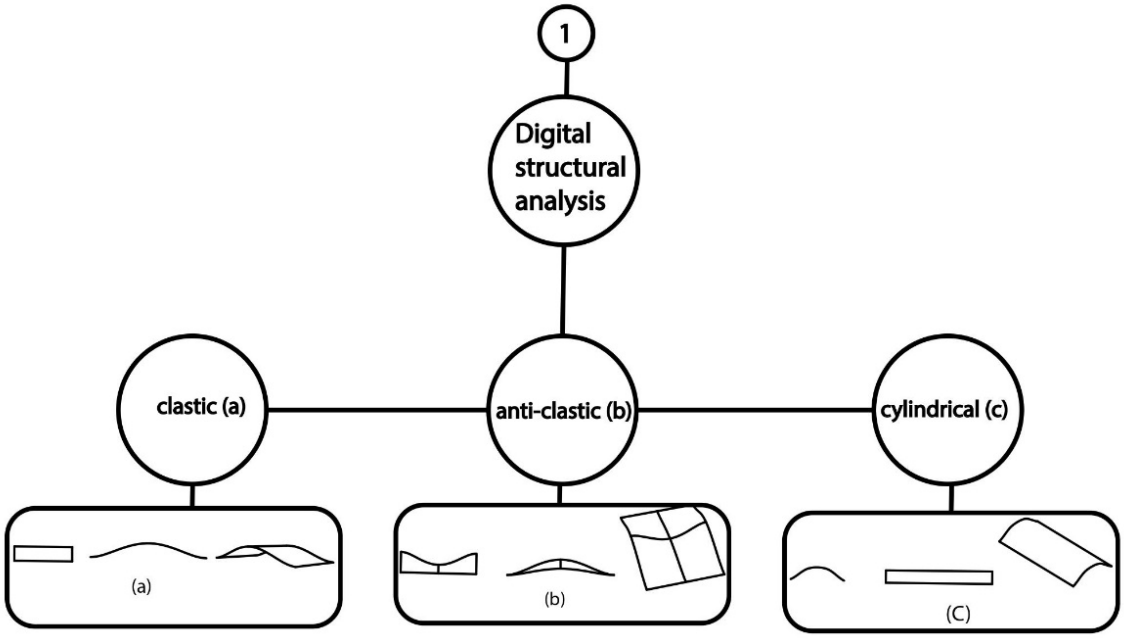

Figure 3.3 the general diagram of the digital structural analysis.

The software Grasshopper/ Karamba has a feature that allows the users to implement material properties, supports, and loads as an input of the test. In this research, the values below were used to test the structures:

1. **Material properties:**
    - **a.** Carbon fiber longitudinal modulus E1 :17 GPa.
    - **b.** Carbon fiber transverse modulus E2 : 17 GPa.
    - **c.** In Plane shear modulus G12: 33 GPa.
    - **d.** Coefficient of thermal expansion in the first material direction Alpha T1 : 2.15 E-6.

e. Coefficient of thermal expansion in the second material direction Alpha T2: 2.15 E-6.

f. Material type orthotropic:

2. **Loads:**

a. Vertical loads: -9.832 in Z axis.

b. Horizontal loads: -4.152 in X axis.

3. **Cross section:**

a. Heights: 4.

b. Elems|Ids: shell.

The above values produced specific number of curves, and the position of the lines and its equidistance, these parameters were controlled parametrically by different components. Figure 3.4 below shows the carbon fiber properties values assigned to Grasshopper/Karamba definition.

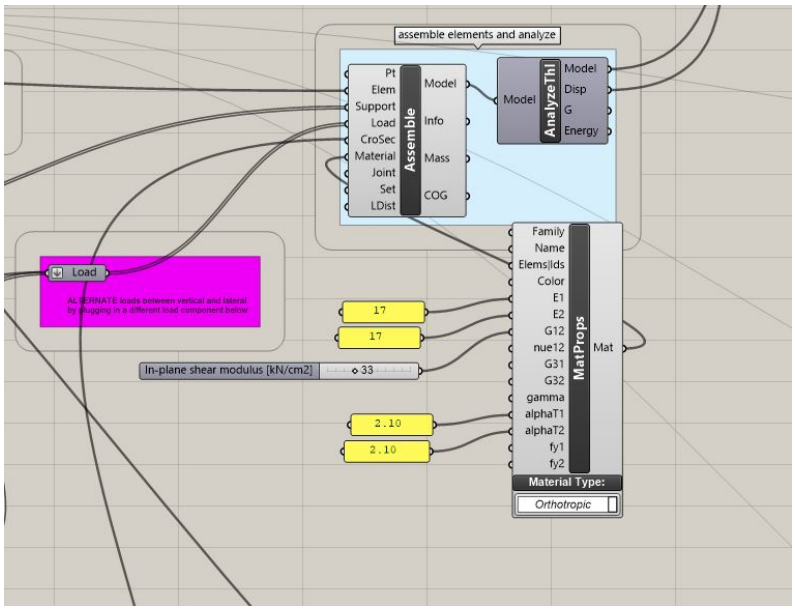

Figure 3.4 Material properties component has values that should be assigned to karamba/Grasshopper definition.

The result of the structural investigation generated 6 different models. Figure 3.5 shows the difference between force-flow and principal stress lines for a shell with zero Gaussian curvature. Figure 3.6 shows the force-flow and principal stress lines for a shell with positive Gaussian curvature. Figure 3.7 shows the force-flow and principal stress lines of negative Gaussian generated from Karamba.

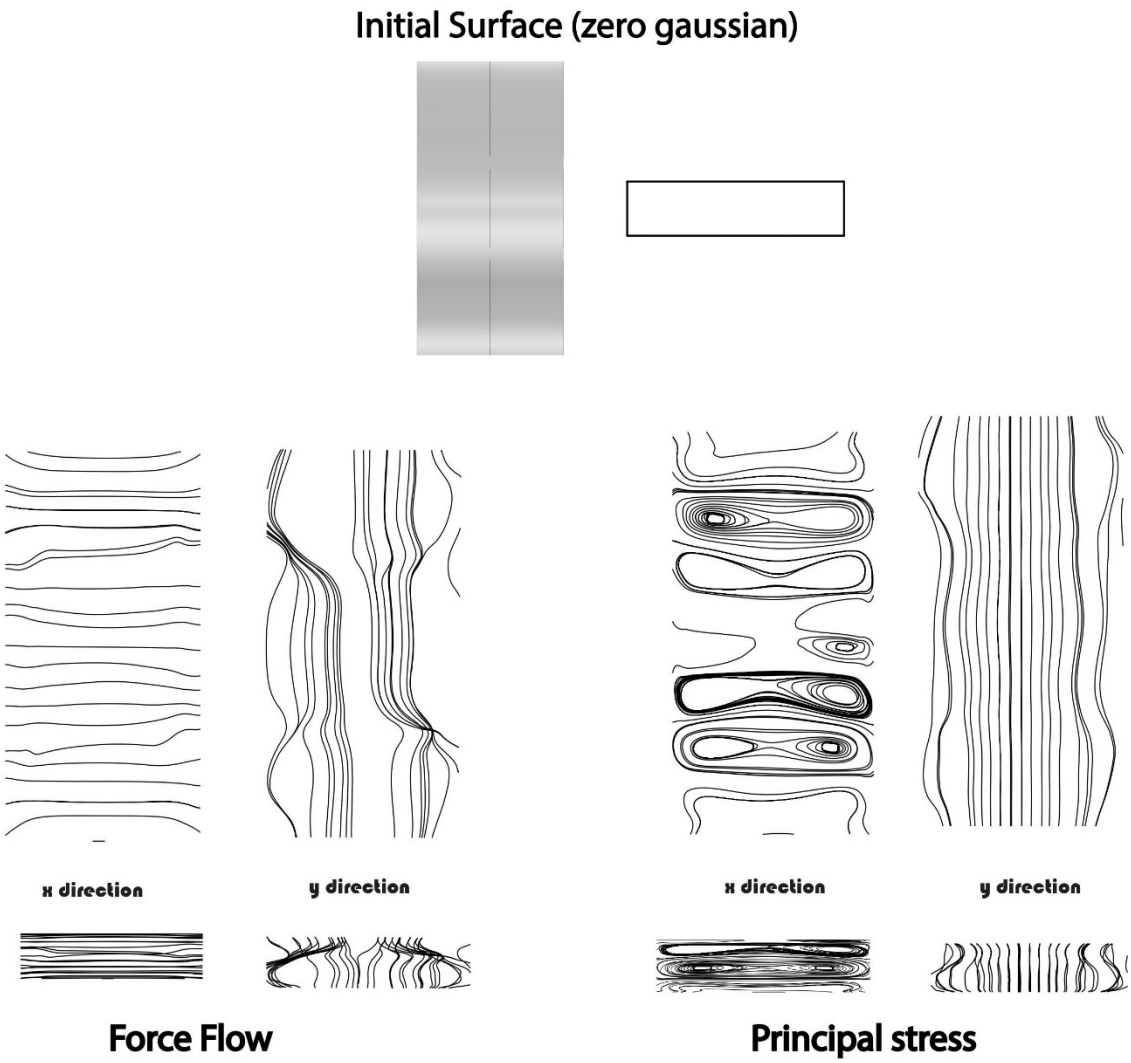

Figure 3.5 The force-flow and principal stress lines of zero Gaussian generated from Karamba.

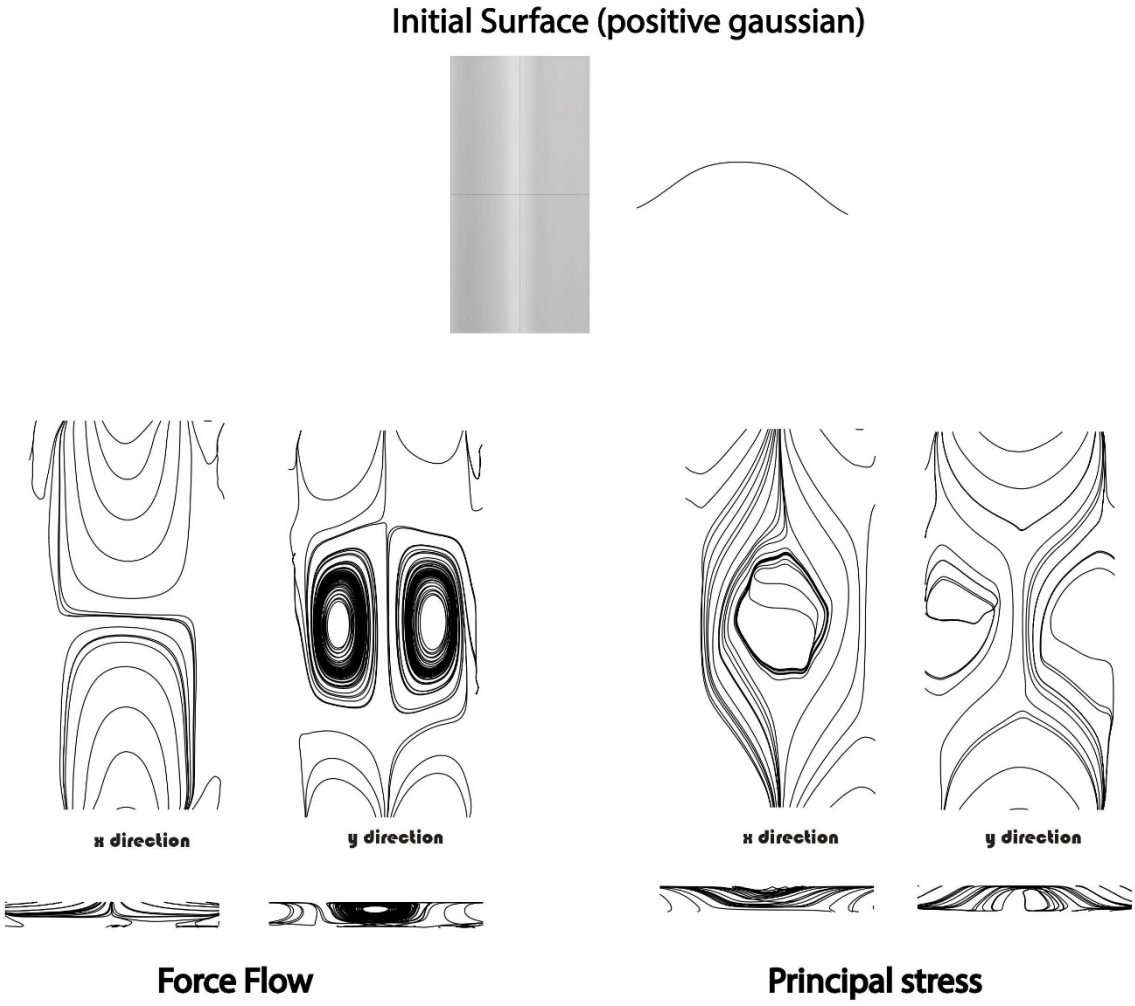

Figure 3.6 the force-flow and principal stress lines of positive Gaussian generated from Karamba.

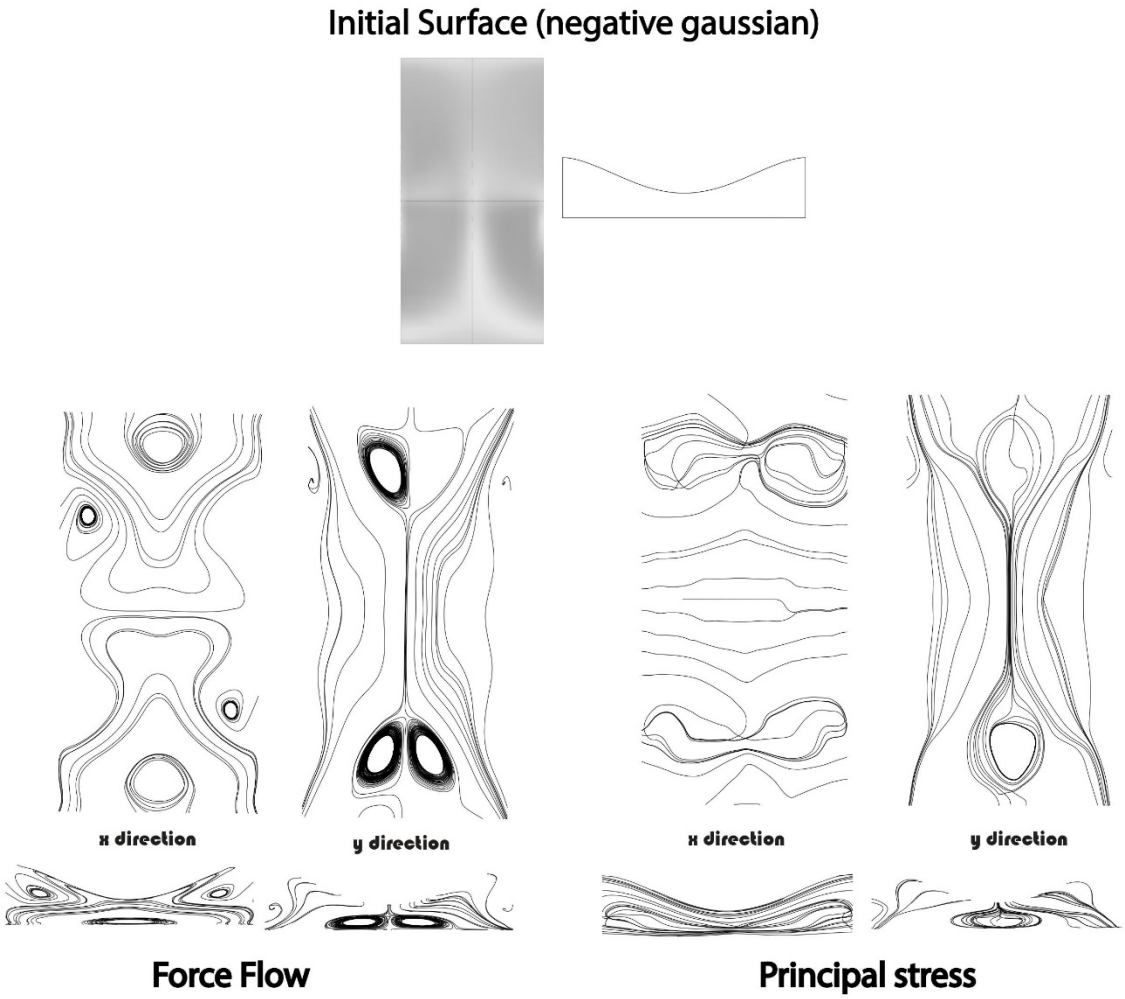

Figure 3.7 the force-flow and principal stress lines of negative Gaussian generated from Karamba.

3.1.1 Force-Flow Lines

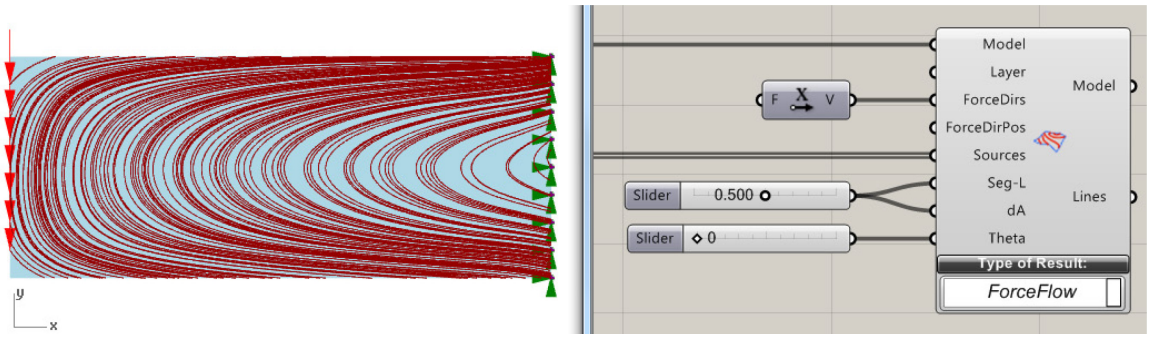

Figure 3.8 the flow lines in horizontal direction (Preisinger, 2016) Retrieved from https://www.karamba3d.com/wp-content/uploads/downloads/2012/04/KarambaManual_0_9_084.pdf

Preisinger describes force-flow as "lines that represent the load distribution in the structure" (Preisinger, 2016). Figure 3.8 shows the force-flow lines in the horizontal direction related to shear or normal stress created by the Karamba component. Preisinger says, "At the upper and lower side of the beam, the force flow represents the maximum normal stress, so the resultant of the forces is nearly horizontal" (Preisinger, 2016). In the middle, the only force represented is shear force (Preisinger, 2016). The input of the component in Karamba/Grasshopper contains the following options:

- Model: Clemens Preisinger says that the model is the shape we want to generate from FF lines (Preisinger, 2016).
- ForceDirs: Clemens Preisinger says that it is a vector or a list of vectors that define the direction projected on each element. In this thesis, X and Y directions were chosen for the optimum analysis and to rigidify the fibers (Preisinger, 2016).
- Source: defined by Clemens Preisinger as the original points on the surface of the shell where FF-lines can be generated from (Preisinger, 2016). The more points we have, the more subdivisions and lines generated as shown in Figure 3.9, Figure 3.10 and Figure 3.11 (Preisinger, 2016).

- Eg-L: Clemens Preisinger says that eg-L represent the length of the segments of the FF-lines (Preisinger, 2016).
- dA: According to Clemens Preisinger, dA is the maximum deferential angle between two adjacent pieces of an FF-line (Preisinger, 2016).
- Theta: According to Clemens Preisinger, "Theta is an input were we can define an angle between the FF-lines and those lines output at the Line-output plug. The angle is in [deg] and defaults to zero" (Preisinger, 2016).

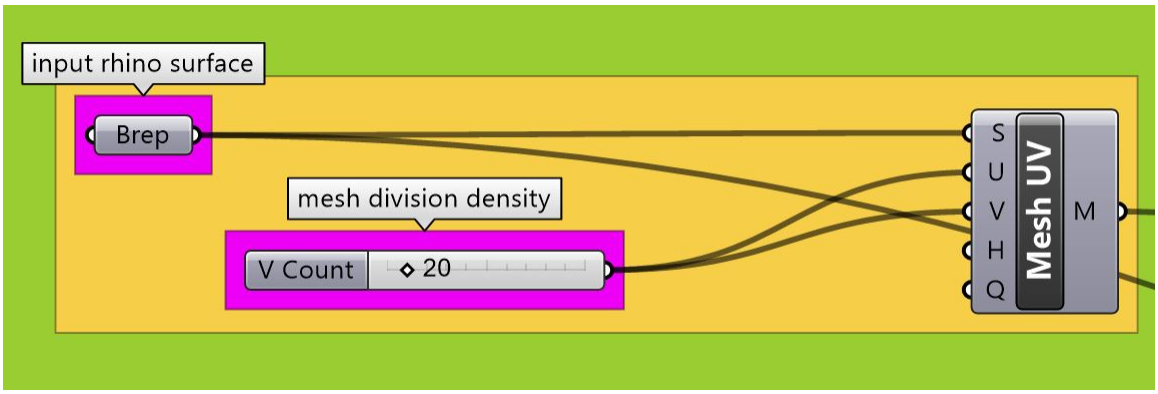

Figure 3.9 A screenshot of karamba source points, V count on the left is set on 20 (mesh division density). https://www.karamba3d.com/wp-content/uploads/downloads/2012/04/KarambaManual_0_9_084.pdf

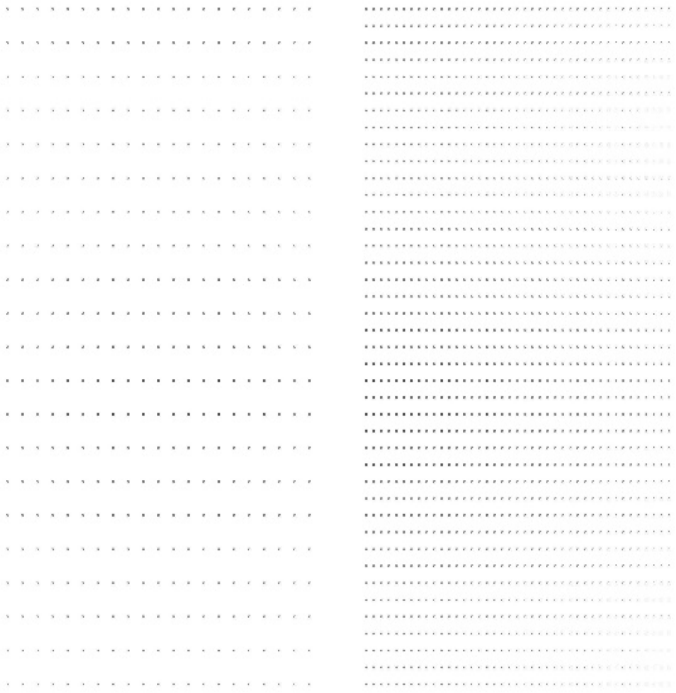

Figure 3.10 Mesh division density and its implication on the force lines. The right image shows the points related to mesh division density generated by Grasshopper

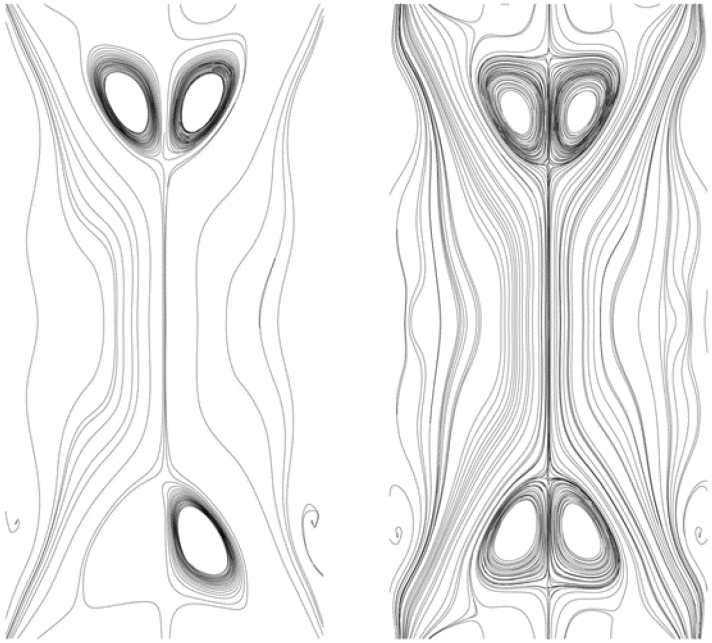

Figure 3.11 The difference between force-flow in Y direction, less subdivided surface (left) as opposed to more subdivided (right).

3.1.2 Principal-Stress Lines

Preisinger describes Principal stress (PS) as “lines that are tangent to the principal stress directions” (Preisinger, 2016), as shown in Figure 3.12. According to Preisinger “In the case of a cantilever, PS lines run either parallel or at a right angle to the free boundaries”. (Preisinger, 2016).

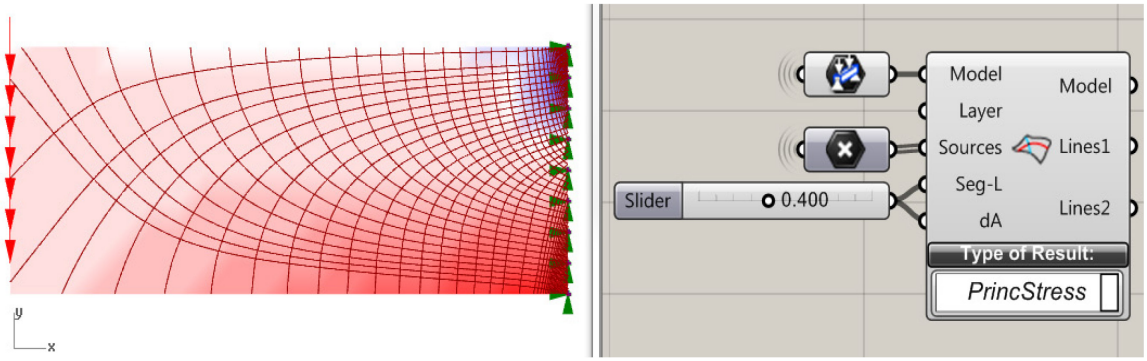

Figure 3.12 According to Preisinge “Principal stress lines are tangent to the first and second principal stress direction. The coloring reflects the level of material utilization” (Preisinger, 2016). Retrieved from: https://www.karamba3d.com/wpcontent/uploads/downloads/2012/04/KarambaManual_0_9_084.pdf

3.2 Experimental Set-Up

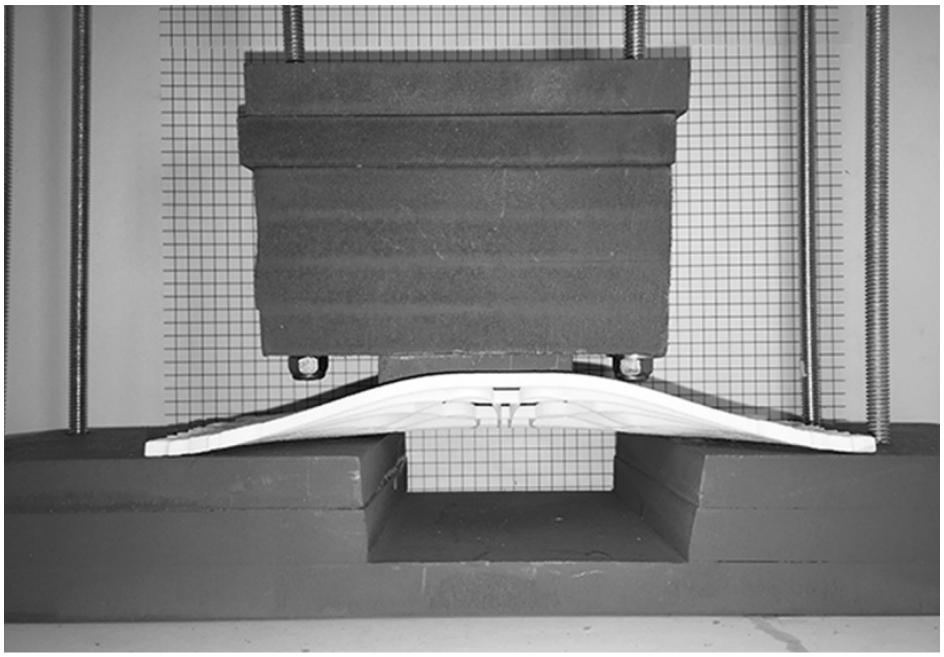

Figure 3.13 shows a photograph of the experiment

A key question of this thesis involves identifying the best method in which to translate structural information to a weave pattern to maximize structural performance. In service of this goal, a set of experiments were proposed to test different methods of weave pattern creation. Specifically, to test the structural performance difference between patterns derived from force-flow lines verses principal stress, three different shell forms were explored.

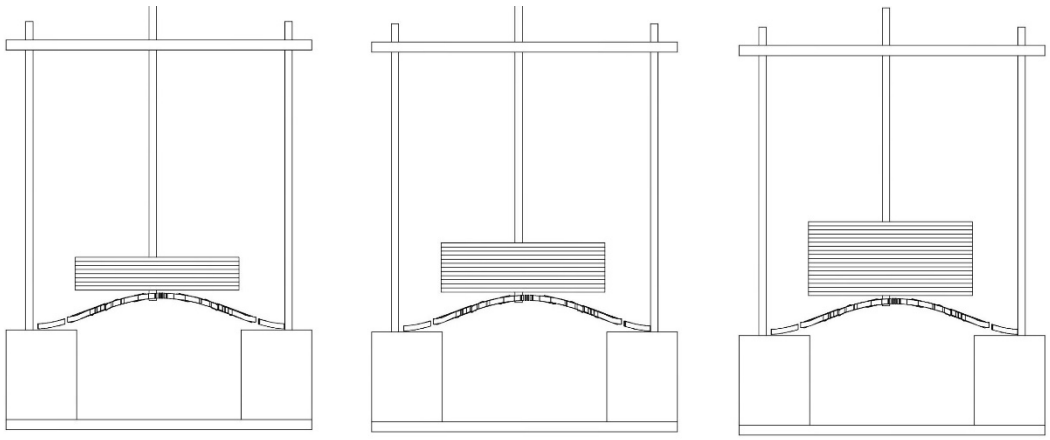

Figure 3.14 shows a diagram of the experiment

A grid of lines was built on the wall of the foam board model to measure the displacements, and weights of wood were added to perform the displacement as shown in Fig 3.13. Figure 3.14 shows the different weights tested in this thesis, which is 220grames, 330 gr, and 495gr.

The third step was to test different structures (Form 1-6) employing CFRP and compare each type of weaving pattern generated by Karamba. The physical test consists of increasing the load on the shell form. The maximum displacement before failure was recorded for each weave pattern and form studied as shown in Figure 3.15.

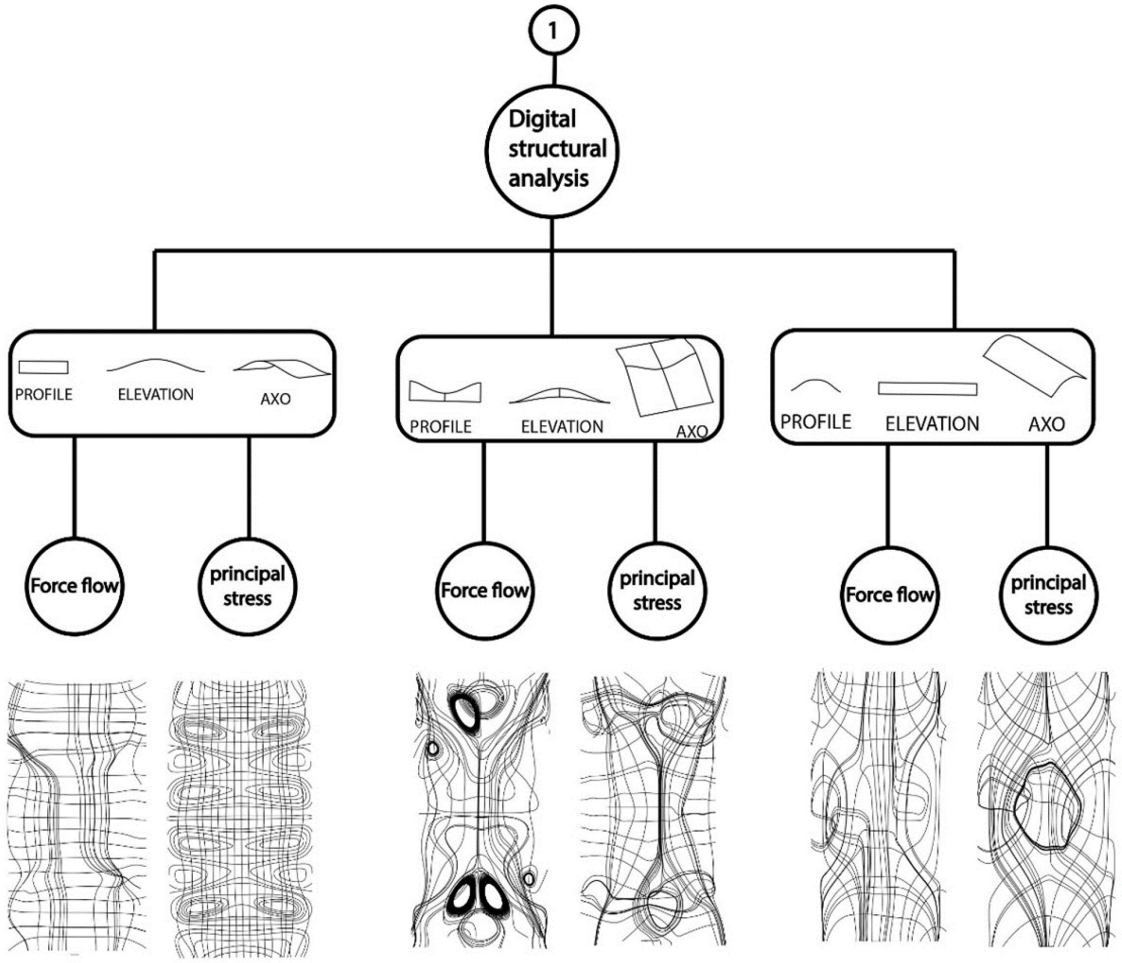

Figure 3.15 summarizes the structural tests of 3 models

3.3 Fabrication

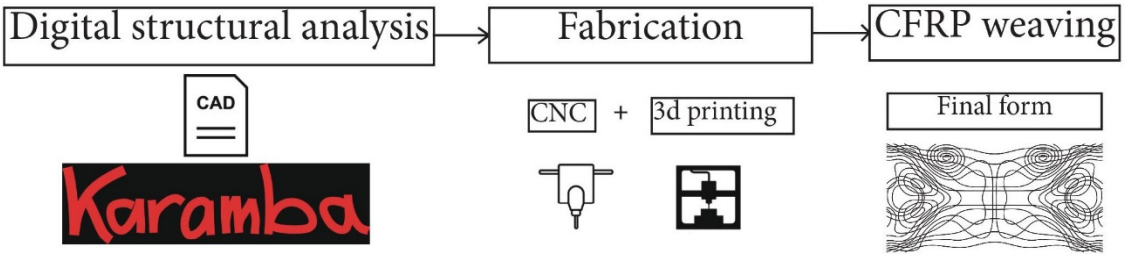

Figure 3.16 *Shows the fabrication process using Subtractive and additive manufacturing processes to validate specific weaving pattern.*

This section describes the fabrication method of the weave patterns developed from structural analysis through two processes. The first process used an additive fabrication technology called selective laser sintering (SLS). This process was the primary process explored in this thesis. SLS was chosen because it is the fastest additive process in the market and provides excellent mechanical properties, such as high strength and stiffness. With the SLS process, different materials can be used, like: nylon, versatile plastic, steel, aluminum, and plastic. It also does not require cleaning or removal of support material, so the designed object can be used promptly. SLS is therefore entirely self-supporting and allows highly complex geometry to be built. Figure 3.16 shows the fabrication process diagram using Subtractive and additive manufacturing processes. The second process uses subtractive fabrication and the 3-axis CNC router; it is explained in **Chapter 6. APENDIX A**. It is important to note that this process is not validated in this thesis, but it is left for future investigations.

3.3.1 Additive Fabrication: SLS

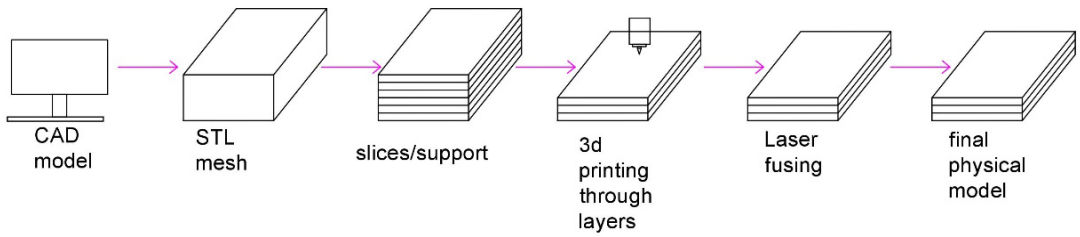

Figure 3.17 The diagram of SLS 3d printing process: first step is the creation of CAD model; stl mesh, then it is 3d printed through layers using laser technique.

The process of 3d printing started with a CAD model. Curves derived from the structural analysis in Grasshopper and Karamba were then offset and extruded with an appropriate thickness for the 3d printing. Figure 3.17 shows the diagram that summarizes the SLS 3d printing process. Before the SLS process could begin, it was necessary to check and prepare the geometry for the weave patterns to be fabricated. This process started by checking mesh integrity and repairing it to ensure the shapes were continuous surfaces with no holes. In this step, online software checked the holes in the mesh, self-intersections, flipped and double triangles, degenerate faces, and overlapping shells. Then, the online software checked that the design was within the maximum bounding box for the 3d printer,

which is 650 mm x 350 mm x 550 mm. It also checked if two separate shells were positioned closer than the minimum clearance.

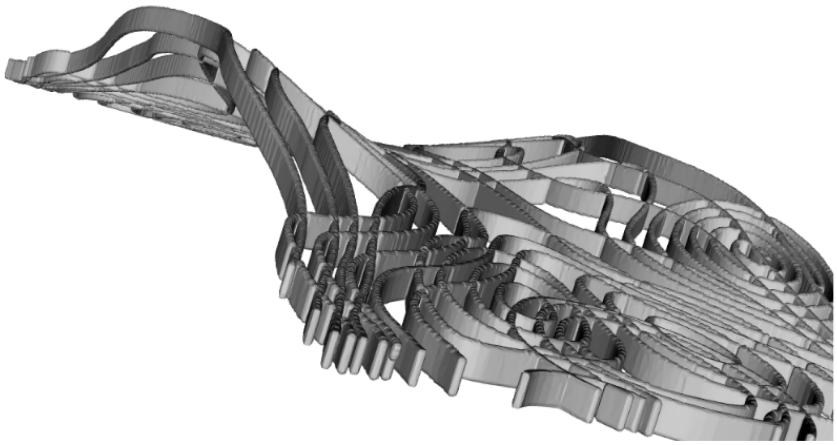

Figure 3.18 A screenshot of the mesh of the 3d print object from Shapeways.

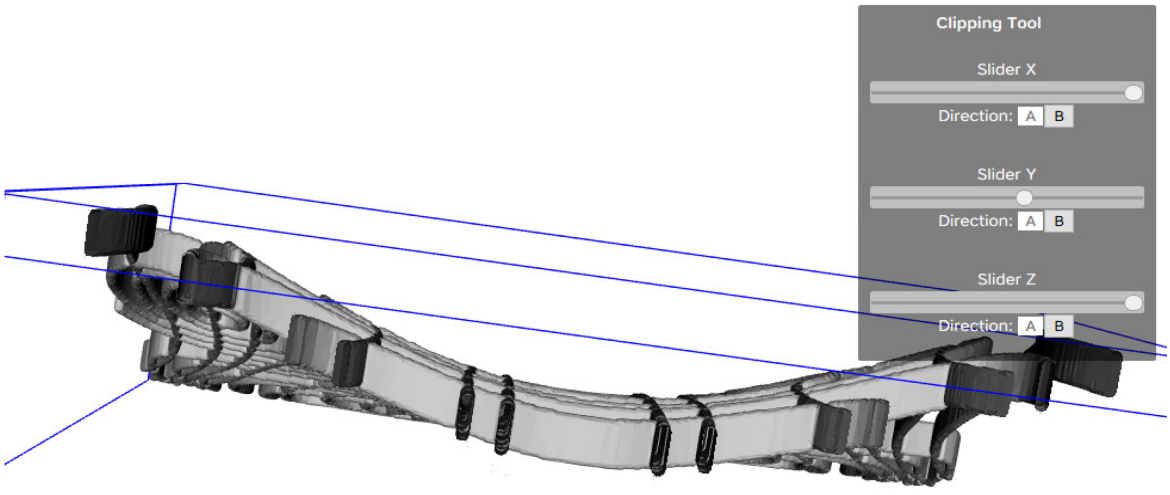

Figure 3.19 shows a screenshot of loose shells. In this step we can check if two separate shells are positioned closer than the minimum clearance.

Chapter 4. Results and Analysis

The structural test started by stacking four wood boards' weights of 220 gram, the second one weighed 330 gram, the third model weighed 495 grams. After the drop test was performed, the highest value of displacement of the force flow derived weave patterns and principal stress patterns was observed in the shell form with negative Gaussian curvature. The shell form with positive Gaussian also has an important displacement in principal stress. The shell form with zero Gaussian curvature had the highest displacement with the force-flow derived weave pattern. Figure 4.1 shows the structural tests performed on the six models.

The data collected from the force-flow experiments showed that there is a large discrepancy of the amount of displacement in the three forms (the average displacement recorded is 4.95 mm). The highest displacement is perceived in the force-flow with 7.1 mm displacement value in the negative Gaussian curvature as shown in table 1, 2, and 3.

The data collected from the principle stress experiments showed that amount of displacement in the three forms was almost identical with a slight variance; see Table 1, 2, 3. The highest displacement of the principle stress weave pattern was 12.1 mm. The recorded positive Gaussian curvature had the highest principal stress displacement.

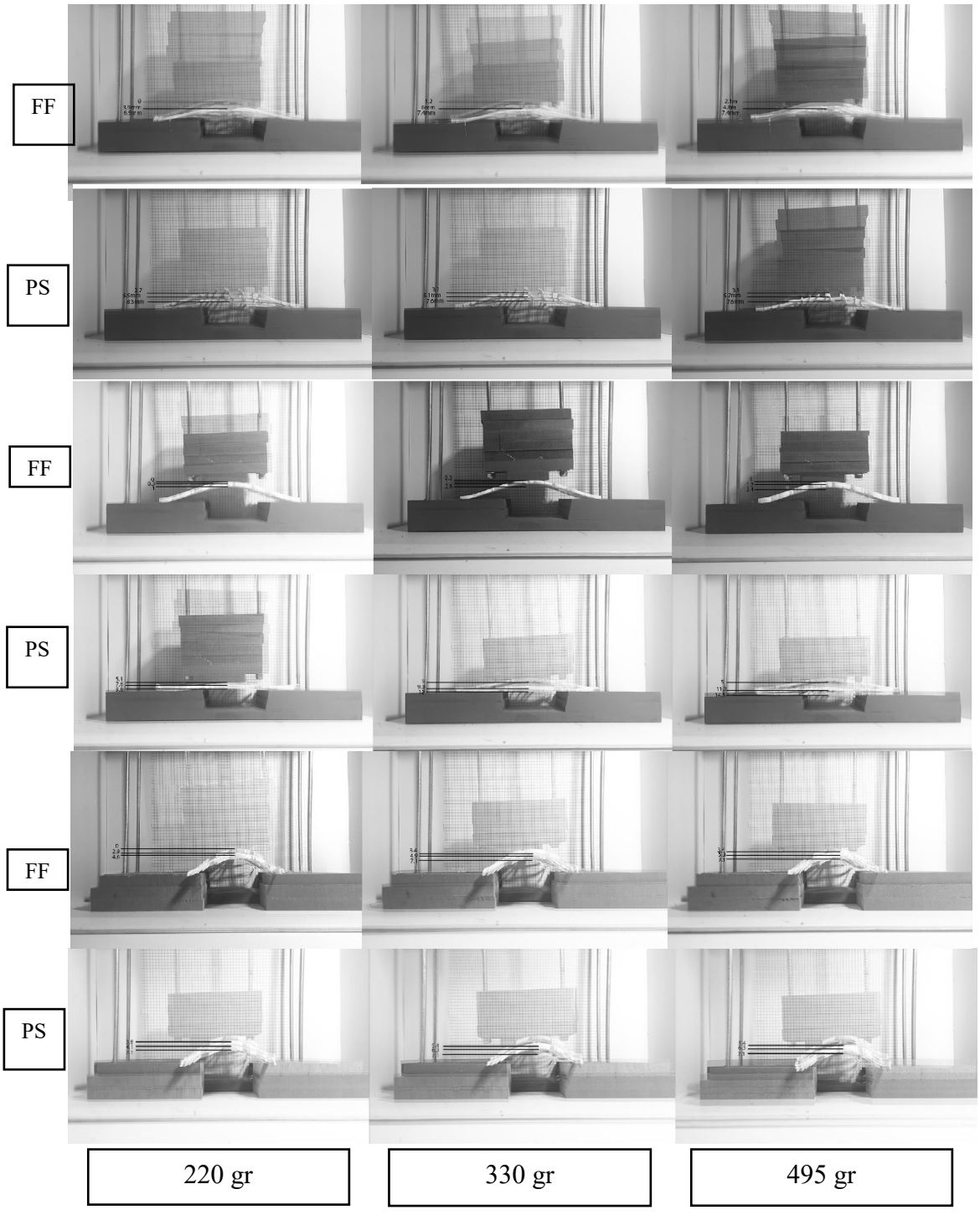

Figure 4.1 The structural tests performed on the six models.

The tables and the charts below summarize the values of displacement found:

Table 1 Negative Gaussian curvature experiment with both force-flow and principal stress.

Weights	Negative Gaussian							
	Force-flow				Principal stress			
	Test 1	Test 2	Test 3	average	Test 1	Test 2	Test 3	average
220gr	0	1.2	2.1	1.1	2.7	3.1	3.1	2.9
330gr	3.9	6	4.8	4.9	5.5	5.1	5.7	5.4
495gr	6.5	7.4	7.4	7.1	8.3	7.6	7.6	7.8

Table 2 Positive Gaussian curvature experiment with both force-flow and principal stress.

Weights	Positive Gaussian							
	Force-flow				Principal stress			
	Test 1	Test 2	Test 3	average	Test 1	Test 2	Test 3	average
220gr	0	0.3	1	0.43	5.1	5	5	5.03
330gr	0.3	1.1	1.7	1.03	7.6	9.3	11.2	9.4
495gr	1	2.8	3.4	2.4	9.8	12	14.5	12.1

Table 3 Zero Gaussian curvature experiment with both force-flow and principal stress.

Weights	Zero Gaussian							
	Force-flow				Principal stress			
	Test 1	Test 2	Test 3	average	Test 1	Test 2	Test 3	average
220gr	0	3.4	3.4	2.3	3.8	5.4	5.4	4.8
330gr	2.9	4.9	5.3	4.4	4.1	6.3	6.3	5.6
495gr	4.6	7.1	7.1	6.3	7.1	7	7.1	7.1

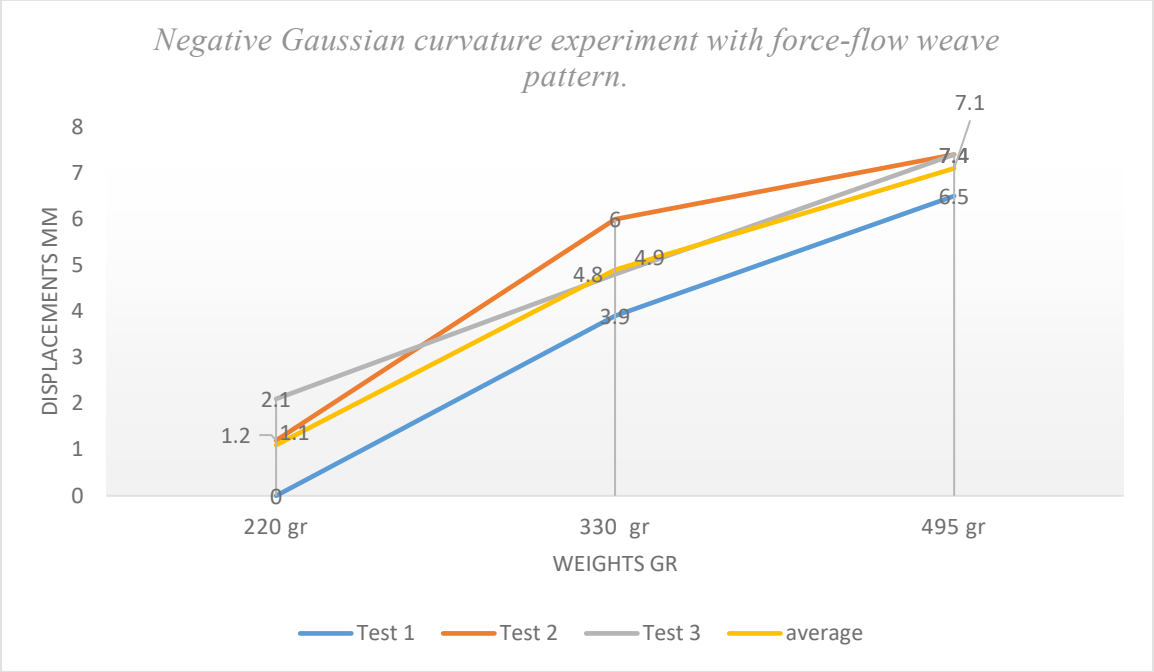

Figure 4.2 Negative Gaussian curvature experiment with force-flow weave pattern.

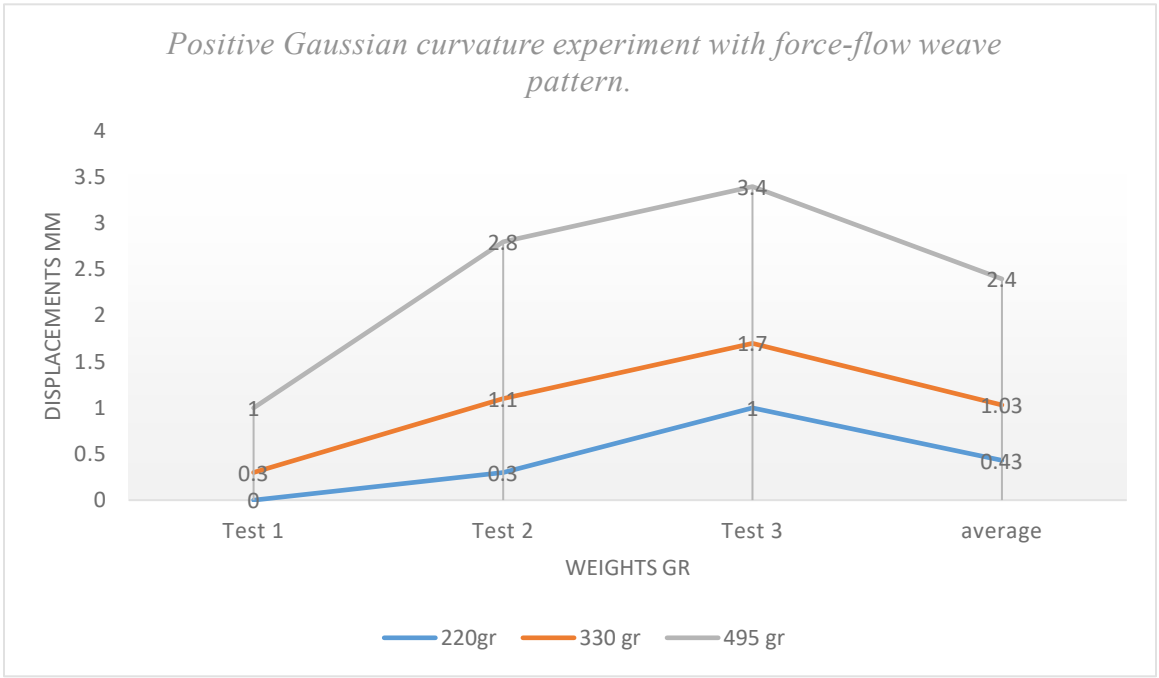

Figure 4.3 Positive Gaussian curvature experiment with force-flow.

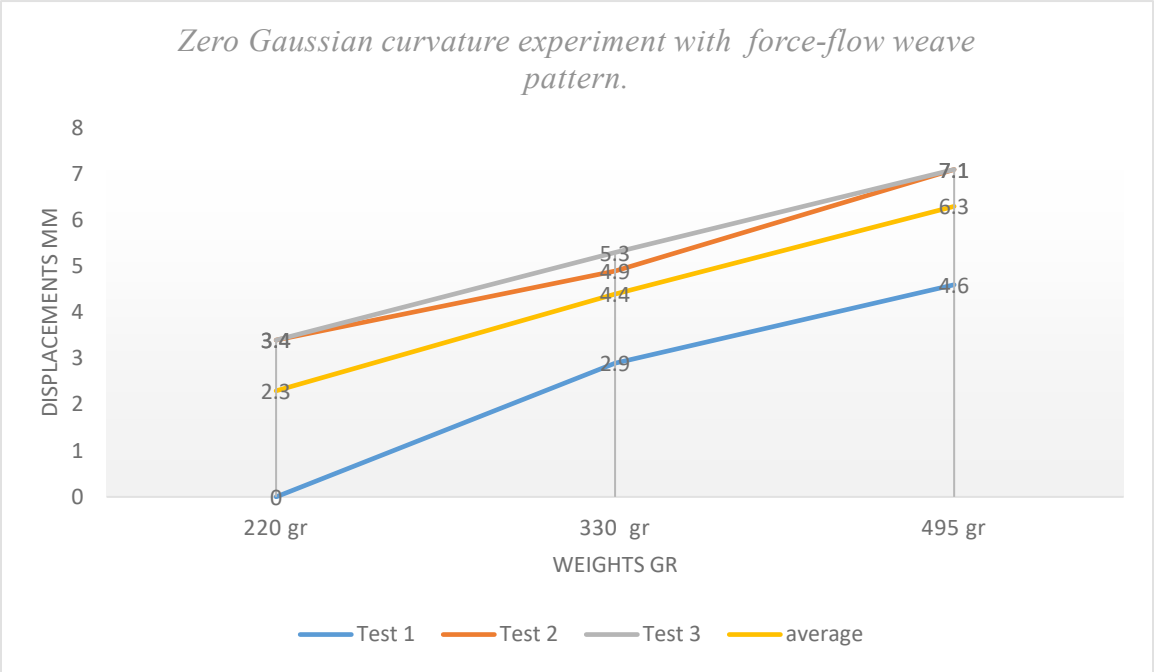

Figure 4.4 Zero Gaussian curvature experiment with force-flow weave pattern.

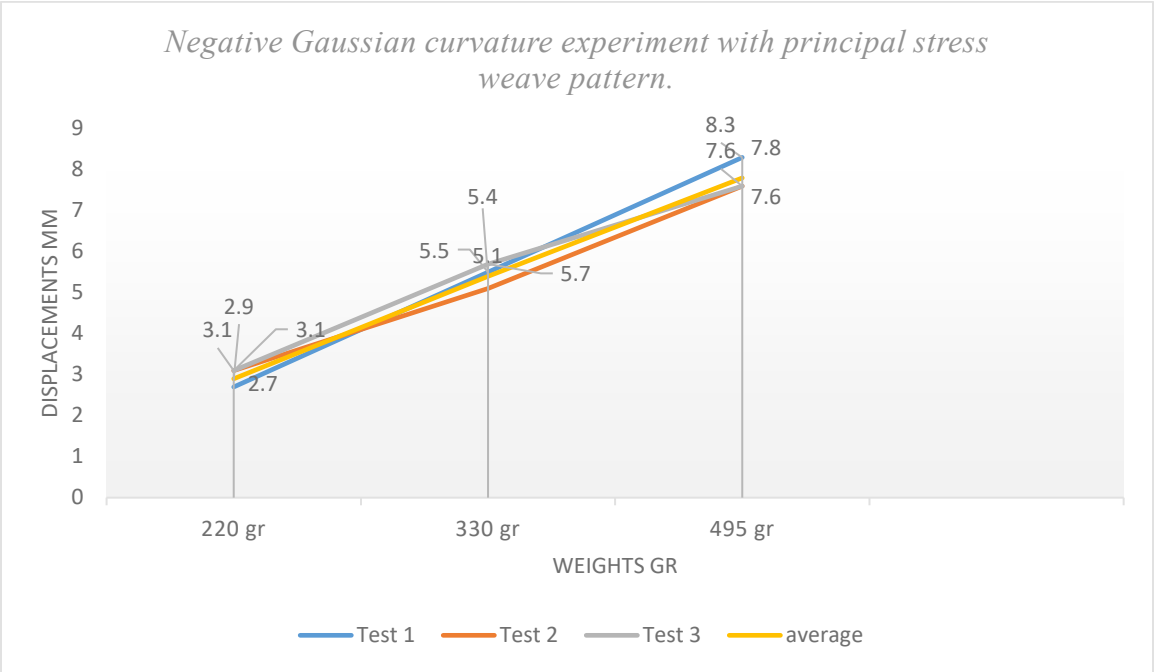

Figure 4.5Negative Gaussian curvature experiment with principal stress weave pattern.

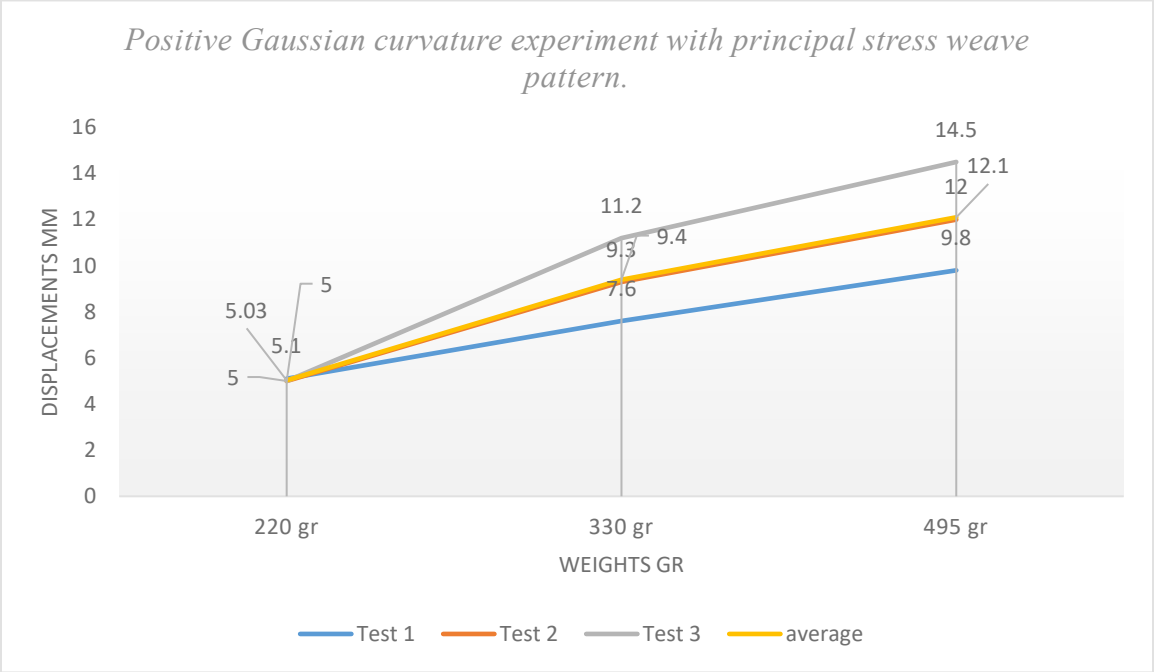

Figure 4.6 Positive Gaussian curvature experiment with principal stress weave pattern.

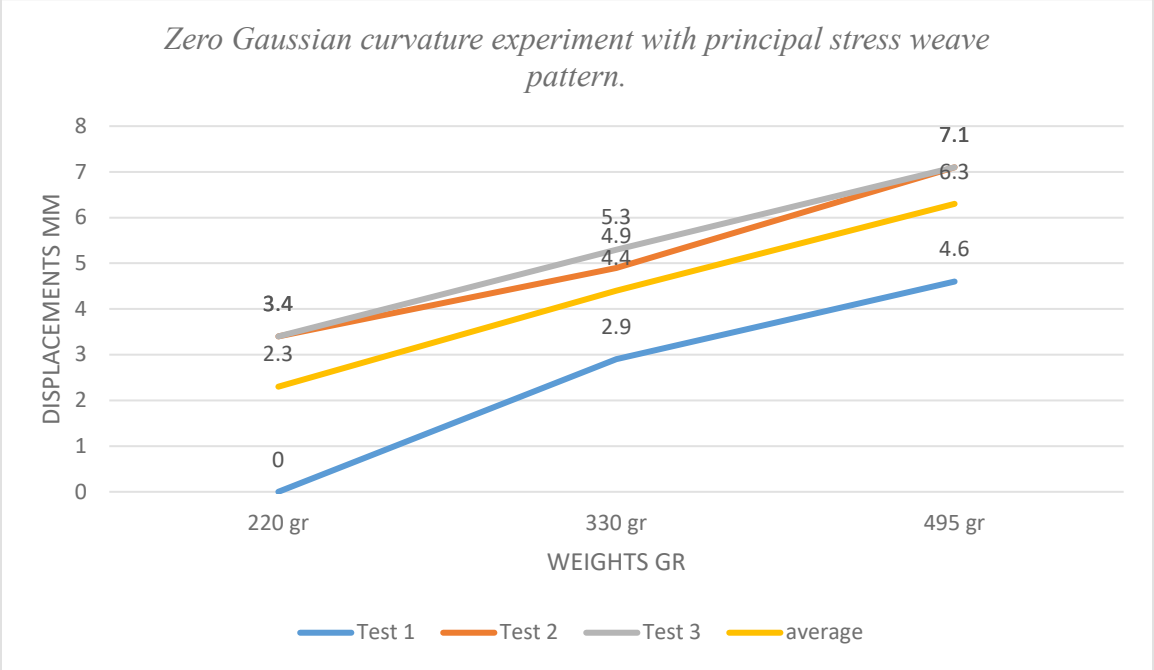

Figure 4.7 Zero Gaussian curvature experiment with principal stress weave pattern.

The combined data from the test shows that the negative Gaussian (anticlastic double curvature) was the most vulnerable form because the surface with Gaussian curvature was negative at all points, and anticlastic double curvature has complex configuration pattern for the force-flow and principal stress alike. The force-flow pattern performs better than the principle stress because the average deflection of the structural tests of force-flow weave pattern in the six models is 3.33 mm, while the average deflection of the structural tests of principal stress weave pattern in the six models is 6.7 mm. Consequently, the force-flow is the information we should implement when we design more efficient force-driven weave pattern in shell structures.

Chapter 5. Conclusions and Future Work

This thesis explored force derived weave patterns for shell structures based on FEA structural analysis. It contributes knowledge in translating digital structural analysis into structurally optimal weave patterns for carbon fiber reinforced polymer shell structures. The average deflection of the structural tests of force-flow weave pattern in the six models is 3.33 mm, while the average deflection of the structural tests of principal stress weave pattern in the six models is 6.7 mm. The force-flow weave patterns are the most efficient patterns, it was validated through physical tests, and this research provides valuable insight for other researchers in the discipline of architecture.

Although this thesis focused on the digital structural analysis and experimented with the additive manufacturing SLS, it is necessary to explore other fabrication processes and materials. Specifically, future research will explore the use subtractive CNC processes to make molds and carbon fiber as the primary material for the weave pattern. Additionally, seven-axis robot arms could be used as an alternative technique to the 3-axis CNC router. Moreover, an additional study on weaving could focus on using robotic arms to make the weaving pattern without the fabrication of molds. Therefore, one could use plastic or fabric shells hardened by resin, then apply the weaving directly on the shells.

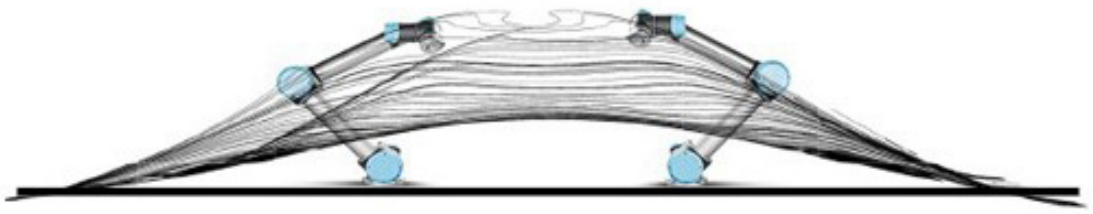

Figure 5-1 shows the routine of the robots' arms that may be implemented in the construction of the weave pattern.

Also, an implementation of C# programming language in Rhino/Grasshopper to automate the weave pattern will be useful because it helps to create a curve friendly path that take into consideration the constraints of the curvature of the surface, the boundaries and the cut depth of the weave pattern. This research omitted certain parameters, such as the size and thickness of the beams generated by Karamba. Therefore, future digital structural analysis work could include these parameters as an input to generate the force flow and principle stress weave patterns by using multi-objective optimization strategies that optimize for these parameters.

Previous research on FRP in the construction of shell structures has exclusively focused on the use of carbon fiber and fiberglass. An alternative material that performs almost similarly, and is much cheaper, is basalt fiber-reinforced polymers (BFRP). Future research in this area will include a comparative study of different types of CFRP and BFRP. Furthermore, to validate which weave patterns perform best, it is necessary to perform physical structural tests on carbon fibers structure rather than 3D printed models because each type of carbon fiber has distinct properties.

REFERENCES

Adriaenssens, Sigrid, Philippe Block, Diederik Veenendaal, and Chris Williams, eds. *Shell Structures for Architecture: Form Finding and Optimization*. Routledge, 2014.

Berardi, Umberto, and Nicholas Dembsey. "Thermal and Fire Characteristics of FRP Composites for Architectural Applications." Polymers 7, no. 11 (2015): 2276-2289.

Bhooshan, Shajay, Vishu Bhooshan, Ashwin Shah, Henry Louth, and David Reeves. "Curve-folded form-work for cast, compressive skeletons." In *Proceedings of the Symposium on Simulation for Architecture & Urban Design*, pp. 221-228. Society for Computer Simulation International, 2015.

Blonder, Arielle, and Yasha Jacob Grobman. "Alternative Fabrication Process for Free-Form FRP Architectural Elements Relying on Fabric Materiality Towards Freedom from Molds and Surface Articulation." (2015).

Dörstelmann, Moritz, Stefana Parascho, Marshall Prado, Achim Menges, and Jan Knippers. "Integrative computational design methodologies for modular architectural fiber composite morphologies." In *Design agency, proceedings of the 34th annual conference of the association for computer aided design in architecture (ACADIA), Los Angeles*, pp. 219-228. 2014.

Doerstelmann, Moritz, Jan Knippers, Valentin Koslowski, Achim Menges, Marshall Prado, Gundula Schieber, and Lauren Vasey. "ICD/ITKE research pavilion 2014–15: Fibre placement on a pneumatic body based on a water spider web." *Architectural Design* 85, no. 5 (2015): 60-65.

Kim, Simon. "Composite Systems for Lightweight Architectures."

Menges, A. "Material Performance-Fibrous Tectonics & Architectural Morphology." Harvard University GSD, Cambridge (2016).

Preisinger, C. "Karamba–parametric structural modeling, user manual for version 1.0. 3." (2013).

STERN, A. "The Para-Pavilion: towards a new aesthetics of parametrically designed pavilions." The Human (2015).

Tam, K. M. M., and C. Mueller. "Stress Line Generation for Structurally Performative Architectural Design." In Proceedings of the Association for Computer Aided Design in Architecture (ACADIA) Conference, Cincinnati, Ohio, US, vol. 3. 2015.

VAN, THOMAS, MORITZ DÖRSTELMANN KAMP, and TOMY DOS SANTOS ROLO. "Beetle Elytra as Role Models for Lightweight Building Construction."

Vasey, Lauren, Ehsan Baharlou, Moritz Dörstelmann, Valentin Koslowski, Marshall Prado, Gundula Schieber, Achim Menges, and Jan Knippers. "Behavioral design and adaptive robotic fabrication of a fiber composite compression shell with pneumatic formwork." In Computational ecologies: design in the anthropocene, Proceedings of the 35th annual conference of the Association for Computer Aided Design in Architecture (ACADIA), University of Cincinnati, Cincinnati, OH, pp. 297-309. 2015.
Weller, W. M. "Form-Finding, Force and Function: a Thin Shell Concrete Trolley Barn for Seattle's Waterfront." (2010).

Websites:

"CIAB PAVILLION.". Accessed May27, 2018. https://www.karamba3d.com/projects/ciab-pavilion

"SHAPEWAYS ". Accessed May 27, 2018. https://www.shapeways.com/

"THINKPARAMETRIC". Accessed May27, 2018. https://thinkparametric.com/

MARK FORNES. Accessed May 27, 2018. https://theverymany.wordpress.com/at/zaha-hadid-architects/

Chapter 6. APENDIX A

Another part of the fabrication investigated in this research was the subtractive fabrication: CNC Routing. The section below details the process of the subtractive fabrication using 3-axis CNC machine.

6.1 Subtractive Fabrication: CNC Routing

Subtractive fabrication in the form of CNC routing was used as a second fabrication process to create woven shell forms. This process was chosen because it saves on fabrication costs and can also produce large-scale prototypes that would be impossible with additive processes like SLS. However, the 3-axis CNC has limitations, such as the number of axes and the fact that the router cannot move or rotate to make undercuts. Before starting the routing process, the curves derived from the structural analysis were rationalized and reduced to make the curves equidistant and to ensure that they did not overlap as shown in Figure 6.2.

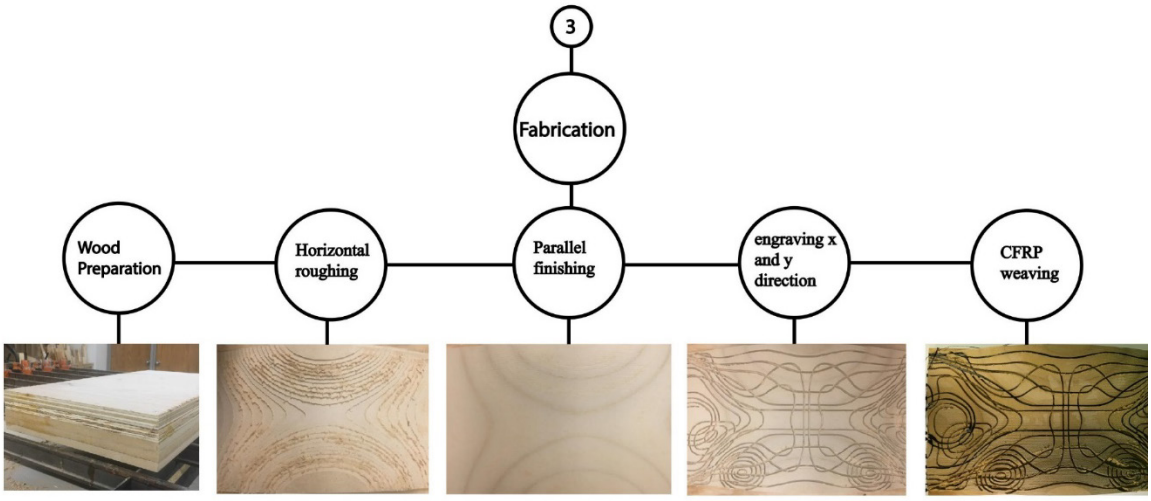

Figure 6.1 The process of subtractive manufacturing

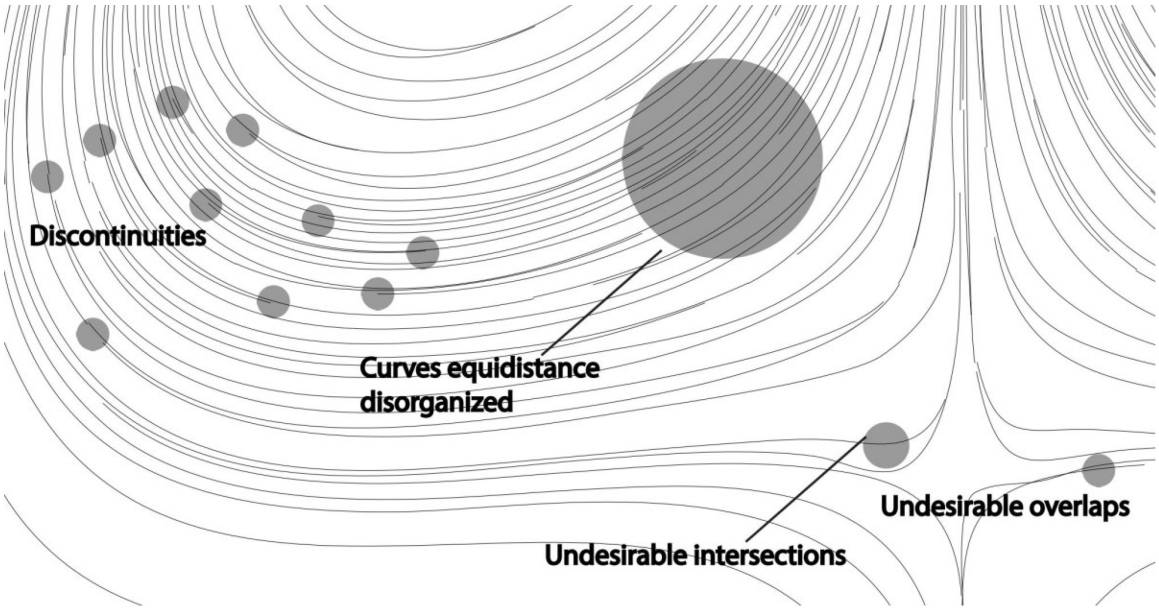

Figure 6.2 The common problems found in using force-flow and principal stress lines directly generated by Karamba.

To fabricate the formwork for my design, Rhinocam 2016 was used to create the routing cut file. The process comprised four machining operations:

Horizontal roughing: In this step, a flat-mill 0.5” tool bit was used to remove the major part of the wood as shown in Figure 6.3.

Figure 6.3 Horizontal roughing: using the CNC.

Parallel finishing: In this step, the tool bit used is a ball mill 0.25” to clean and smooth the surface as shown in Figure 6.4.

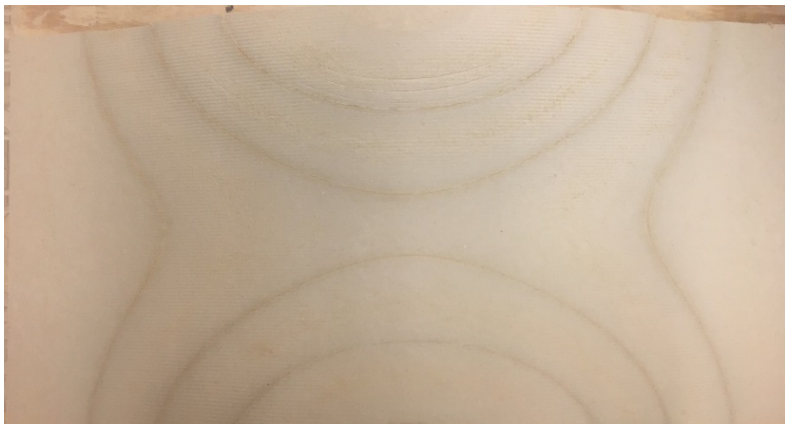

Figure 6.4 Parallel finishing: using the CNC.

Engraving x-direction: In this step, the tool used is a ball-mill 0.125” to engrave the total cut depth which is 0.25”. The cut depth of the first layer of the curves is 0.0625”, so it was necessary to make four rounds to reach the total 0.25” depth.

Engraving y-direction: this step is a repetition of the above but with different curves in the y-direction. Figure 6.5 below shows this last step.

shows a diagram of the summary of steps of the CNC routing process.

Figure 6.5 *The final step of the CNC, it shows engraving x and y directions.*

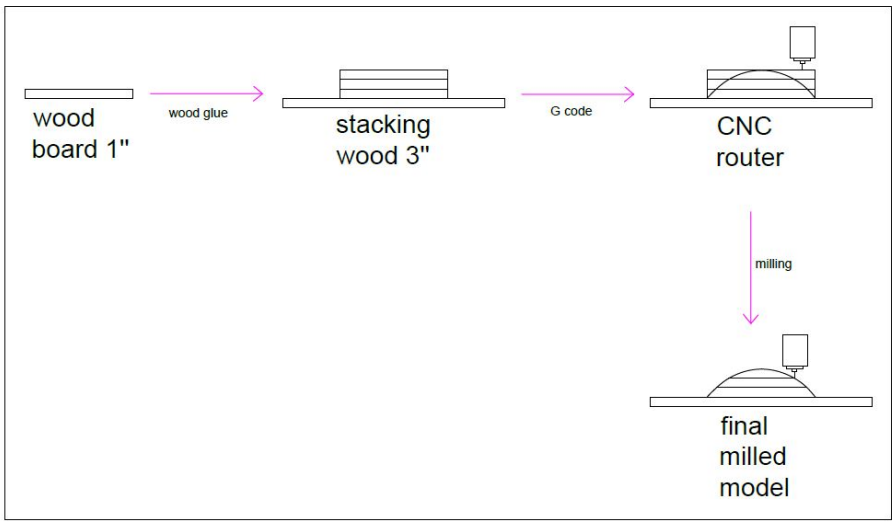

Figure 6.6 The essential steps of the routing process.

Carbon Fiber Weaving:

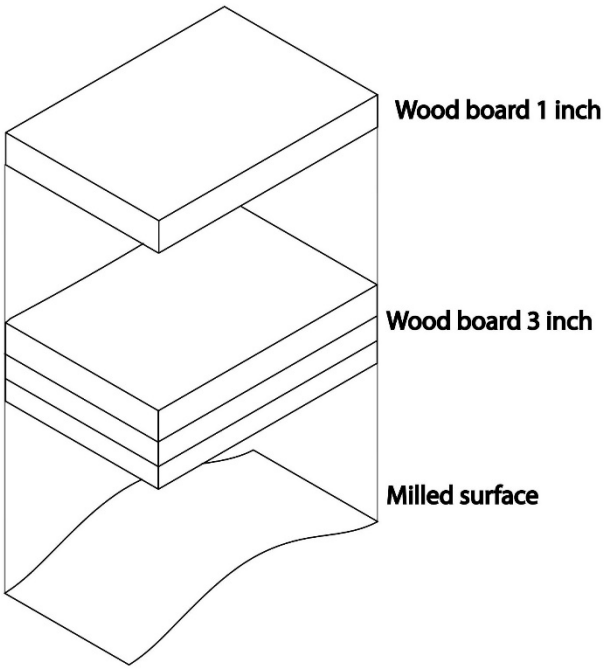

Figure 6.7 The process of preparation of the wood mold 3hx12wx24l''.

Before milling the shapes to create the mold, it was necessary to stack three inches of wood board as shown in Figure 6.6. After the mold was completed for the CNC, screws were added on the edges of the mold to attach the carbon fiber. Then a release agent was added on the engraving pattern to protect the fibers from tearing apart and sticking to the surface of the mold. After this, the carbon fibers were applied by hand and then the mold with the fibers were cured in an industrial oven at 400 F for 1 hour.

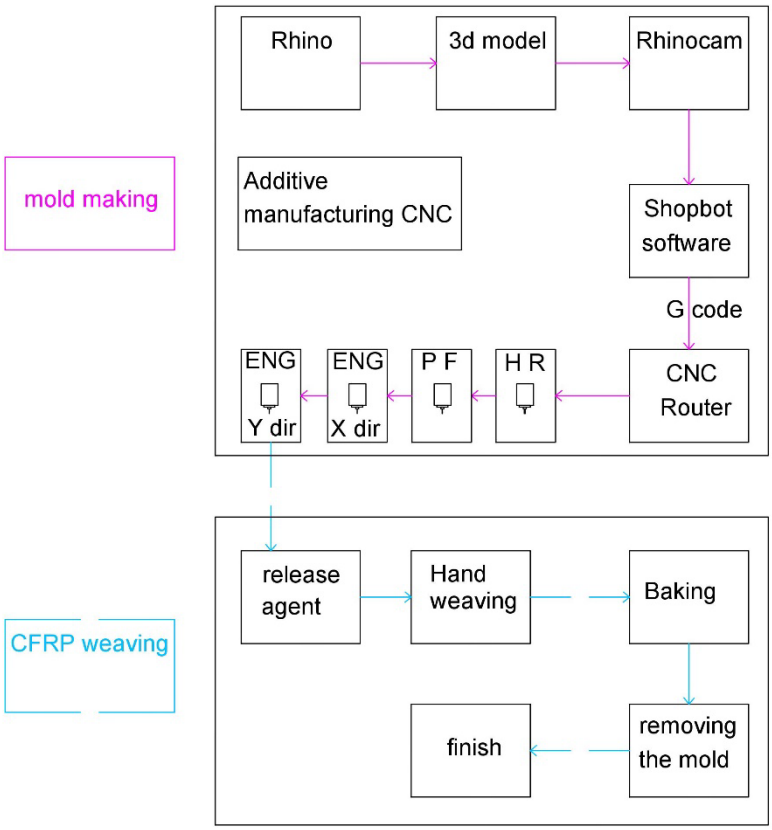

Figure 6.8 The process of subtractive manufacturing, starting from the CAD model to the final physical product.